Glutaredoxin GRXS17 Associates with the Cytosolic Iron-Sulfur Cluster Assembly Pathway[1][OPEN]

Sabrina Iñigo[2], Astrid Nagels Durand[2], Andrés Ritter, Sabine Le Gall, Martin Termathe, Roland Klassen, Takayuki Tohge, Barbara De Coninck, Jelle Van Leene, Rebecca De Clercq, Bruno P. A. Cammue, Alisdair R. Fernie, Kris Gevaert, Geert De Jaeger, Sebastian A. Leidel, Raffael Schaffrath, Mieke Van Lijsebettens, Laurens Pauwels[3], and Alain Goossens[3]*

Department of Plant Systems Biology, VIB, B-9052 Ghent, Belgium (S.I., A.N.D., A.R., S.L.G., B.D.C., J.V.L., R.D.C., B.P.A.C., G.D.J., M.V.L., L.P., A.G.); Department of Plant Biotechnology and Bioinformatics, Ghent University, B-9052 Ghent, Belgium (S.I., A.N.D., A.R., S.L.G., J.V.L., R.D.C., G.D.J., M.V.L., L.P., A.G.); Max Planck Research Group for RNA Biology, Max Planck Institute for Molecular Biomedicine, 48149 Muenster, Germany (M.T., S.A.L.); Institut für Biologie, Fachgebiet Mikrobiologie, Universität Kassel, D-34132 Kassel, Germany (R.K., R.S.); Max Planck Institute of Molecular Plant Physiology, D-14476 Potsdam-Golm, Germany (T.T., A.R.F.); Centre of Microbial and Plant Genetics, Katholieke Universiteit Leuven, B-3001 Leuven, Belgium (B.D.C., B.P.A.C.); Cells-in-Motion Cluster of Excellence (M.T., S.A.L.) and Faculty of Medicine (S.A.L.), University of Muenster, 48149 Muenster, Germany; Department of Medical Protein Research, VIB, B-9000 Ghent, Belgium (K.G.); and Department of Biochemistry, Ghent University, B-9000 Ghent, Belgium (K.G.)

ORCID IDs: 0000-0001-5820-7109 (S.I.); 0000-0001-8849-3812 (S.L.G.); 0000-0002-5618-4633 (M.T.); 0000-0002-9349-5086 (B.D.C.); 0000-0002-4932-8192 (J.V.L.); 0000-0002-4068-1811 (R.D.C.); 0000-0001-8087-4768 (B.P.A.C.); 0000-0002-4237-0283 (K.G.); 0000-0001-6558-5669 (G.D.J.); 0000-0001-9484-5247 (R.S.); 0000-0002-7632-1463 (M.V.L.); 0000-0002-1599-551X (A.G.).

Cytosolic monothiol glutaredoxins (GRXs) are required in iron-sulfur (Fe-S) cluster delivery and iron sensing in yeast and mammals. In plants, it is unclear whether they have similar functions. Arabidopsis (*Arabidopsis thaliana*) has a sole class II cytosolic monothiol GRX encoded by *GRXS17*. Here, we used tandem affinity purification to establish that Arabidopsis GRXS17 associates with most known cytosolic Fe-S assembly (CIA) components. Similar to mutant plants with defective CIA components, *grxs17* loss-of-function mutants showed some degree of hypersensitivity to DNA damage and elevated expression of DNA damage marker genes. We also found that several putative Fe-S client proteins directly bind to GRXS17, such as XANTHINE DEHYDROGENASE1 (XDH1), involved in the purine salvage pathway, and CYTOSOLIC THIOURIDYLASE SUBUNIT1 and CYTOSOLIC THIOURIDYLASE SUBUNIT2, both essential for the 2-thiolation step of 5-methoxycarbonylmethyl-2-thiouridine (mcm^5s^2U) modification of tRNAs. Correspondingly, profiling of the *grxs17-1* mutant pointed to a perturbed flux through the purine degradation pathway and revealed that it phenocopied mutants in the elongator subunit ELO3, essential for the mcm^5 tRNA modification step, although we did not find XDH1 activity or tRNA thiolation to be markedly reduced in the *grxs17-1* mutant. Taken together, our data suggest that plant cytosolic monothiol GRXs associate with the CIA complex, as in other eukaryotes, and contribute to, but are not essential for, the correct functioning of client Fe-S proteins in unchallenged conditions.

A large fraction of plant intracellular iron is incorporated in iron-sulfur (Fe-S) prosthetic groups, which are well suited for electron transfer reactions and are often essential for the catalytic function of several enzymes (Balk and Schaedler, 2014). There are three pathways for the assembly of Fe-S clusters in plants: a mitochondrial, a plastidial, and a cytosolic pathway. The cytosolic Fe-S assembly (CIA) pathway is involved in the maturation of [2Fe-2S] clusters into [4Fe-4S] clusters and is capable of providing [4Fe-4S] clusters to cytosolic and nuclear proteins. Because of the absence of a cytosolic Cys desulfurase, the CIA pathway depends on the integrity of the mitochondrial Fe-S cluster machinery and a functional ABC transporter of the mitochondria (Kispal et al., 1999; Gerber et al., 2004). The three pathways share a common mechanism in which the Fe-S is preassembled on a scaffold protein and then transferred to apoproteins by carriers or targeting factors (Fig. 1A; Couturier et al., 2013; Balk and Schaedler, 2014).

Glutaredoxins (GRXs) together with thioredoxins (TRXs) are thiol oxidoreductases that are able to control the redox state of proteins and are present in most organisms (Herrero and de la Torre-Ruiz, 2007). The yeast GRX proteins Grx3/4 and the mammalian ortholog GRX3/PKC-interacting cousin of TRX (PICOT) have been associated with the CIA pathway and contain themselves [2Fe-2S] clusters (Picciocchi et al., 2007; Haunhorst et al., 2010). Deletion of *Grx3/4* in yeast leads to defects in cytosolic and mitochondrial Fe-S assembly, deregulation of iron homeostasis, and defects in proteins containing di-iron centers (Mühlenhoff et al., 2010). Yeast Grx3/4 and human GRX3 belong to the PICOT protein family and contain one N-terminal TRX and one (Grx3/4) or two (GRX3) C-terminal GRX domains, also known as PICOT homology domains

(Haunhorst et al., 2010). Because they contain only a single Cys residue in their GRX active sites, they are classified as monothiol GRXs. They are conserved and present in a broad range of organisms, including bacteria, yeasts, plants, and mammals (Isakov et al., 2000). Whereas there are other monothiol GRXs present in mitochondria, Grx3/4 and GRX3 are the only nucleocytosolic-localized monothiol GRXs (Herrero and de la Torre-Ruiz, 2007).

The sole class II Arabidopsis (*Arabidopsis thaliana*) nucleocytosolic monothiol GRX is GRXS17, which contains one N-terminal TRX and three C-terminal GRX domains. GRXS17 dimers are capable of associating with three [2Fe-2S] clusters in vitro (Knuesting et al., 2015). Its physiological and molecular role in plants is not well understood (Couturier et al., 2013). GRXS17 function has been associated with protection against oxidative stress in Arabidopsis and thermotolerance in Arabidopsis and tomato (Cheng et al., 2011; Wu et al., 2012; Knuesting et al., 2015). Arabidopsis *GRXS17* loss-of-function plants (*grxs17*) are hypersensitive to heat stress and show alterations in auxin sensitivity and polar transport (Cheng et al., 2011). The molecular function of an association of cytosolic monothiol GRX with Fe-S clusters and the CIA pathway has been a subject of debate, and a role in Fe, Fe-S, or oxidative signaling has been proposed, in addition to a role in delivery or repair of Fe-S clusters (Couturier et al., 2015). Recently, delivery of an Fe-S cluster by human GRX3 to the CIA pathway component DRE2/Anamorsin has been demonstrated (Banci et al., 2015).

Cytosolic tRNAs in eukaryotes carry several chemical modifications, often at the anticodon loop. Uridines at the first position of the anticodon (U_{34}) of tRNAs tK(UUU), tE(UUC), and tQ(UUG) are modified to 5-methoxycarbonylmethyl-2-thiouridine (mcm^5s^2U) in eukaryotes. Furthermore, this evolutionarily conserved modification (Mehlgarten et al., 2010) is essential for unperturbed translation and cellular signaling (Zinshteyn and Gilbert, 2013; Scheidt et al., 2014; Nedialkova and Leidel, 2015). The 2-thiolation (s^2) step of mcm^5s^2U is catalyzed by the UBIQUITIN-RELATED MODIFIER (URM1) pathway and requires the CIA complex in yeast (Nakai et al., 2007; Leidel et al., 2009). The mcm^5 modification is catalyzed by the elongator (ELP) pathway and requires the Elp3/ELO3 catalytic subunit, i.e. a [4Fe-4S] protein (Huang et al., 2005; Paraskevopoulou et al., 2006; Selvadurai et al., 2014), together with the Trm9/Trm112 complex, which is a tRNA methyltransferase necessary for the last step of mcm^5 formation (Kalhor and Clarke, 2003; Chen et al., 2011; Leihne et al., 2011). The presence of the mcm^5 chain is necessary for an effective thiolation of tRNAs (Leidel et al., 2009; Chen et al., 2011). Although in vivo data are scarce, tRNA modifications might have a regulatory function, because certain open reading frames (ORFs) are enriched in codons recognized by modified tRNAs. In yeast, genes involved in the DNA-damage response are enriched in GAA, AAA, and CAA codons and elongator mutants defective in mcm^5s^2 modification are hypersensitive to DNA stress (Chen et al., 2011).

Here, we found the Arabidopsis glutaredoxin GRXS17 to associate with members of the CIA pathway machinery and with several putative Fe-S client proteins, such as XANTHINE DEHYDROGENASE1 (XDH1) and the URM1 pathway components CYTOSOLIC THIOURIDYLASE SUBUNIT1 (CTU1) and CTU2. Accordingly, mutants lacking *GRXS17* showed similar phenotypes, at molecular, cellular, and/or physiological levels, as mutants in genes encoding CIA components or proteins involved in mcm^5s^2 tRNA modification. Our results endorse the association of cytosolic monothiol GRXs with the CIA complex, Fe-S cluster metabolism, and tRNA modification in plants.

RESULTS

GRXS17 Associates with the CIA Complex and Fe-S Proteins

To characterize the role of Arabidopsis GRXS17 and uncover potential links with Fe-S cluster assembly or delivery to proteins, we used tandem affinity purification (TAP; Van Leene et al., 2015). GRXS17 was fused both to an N-terminal and a C-terminal TAP-tag and expressed both in Arabidopsis cell cultures and seedlings under the control of the cauliflower mosaic virus (CaMV) 35S promoter. Copurified proteins included nearly all known core components of the CIA pathway, two known Fe-S proteins, i.e. XDH1 and BolA2, and a number of proteins implicated in tRNA metabolism (Table I; Supplemental Dataset S1). Notably, we identified more GRXS17-interacting proteins when using the C-terminal TAP-tag than when using the N-terminal TAP-tag, suggesting that the position of the tag affects protein folding or that different domains of GRXS17

[1] This work was supported by the Research Foundation Flanders through the projects G005212N and G005312N and a postdoctoral fellowship to L.P.; the Belgian Science Policy Organization for postdoctoral fellowships to S.I. and A.R.; the European Commission Marie Curie Research Training Network (CHIP-ET, FP7-PEOPLE-2013-ITN607880) to M.V.L. and S.L.G.; the Max Planck Society to S.A.L.; the Deutsche Forschungsgemeinschaft SPP1784 "Chemical Biology of Native Nucleic Acid Modifications" to R.K. (KL2937/1-1), R.S. (SCHA750/20-1), and S.A.L. (LE 3260/2-1); and SPP1927 "Iron-Sulfur for Life: Cooperative Function of Iron-Sulfur Centers in Assembly, Biosynthesis, Catalysis and Disease" to R.S. (SCHA750/21-1).

[2] These authors contributed equally to the article.

[3] These authors contributed equally to the article.

* Address correspondence to alain.goossens@psb.vib-ugent.be.

The author responsible for distribution of materials integral to the findings presented in this article in accordance with the policy described in the Instructions for Authors (www.plantphysiol.org) is: Alain Goossens (alain.goossens@psb.vib-ugent.be).

L.P. and A.G. designed the research; S.I., A.N.D., A.R., S.L.G., M.T., R.K., T.T., B.D.C., and R.D.C. performed research; all authors analyzed data; S.I., A.N.D., S.A.L., R.S., L.P., and A.G. wrote the article with help from all authors.

[OPEN] Articles can be viewed without a subscription.

www.plantphysiol.org/cgi/doi/10.1104/pp.16.00261

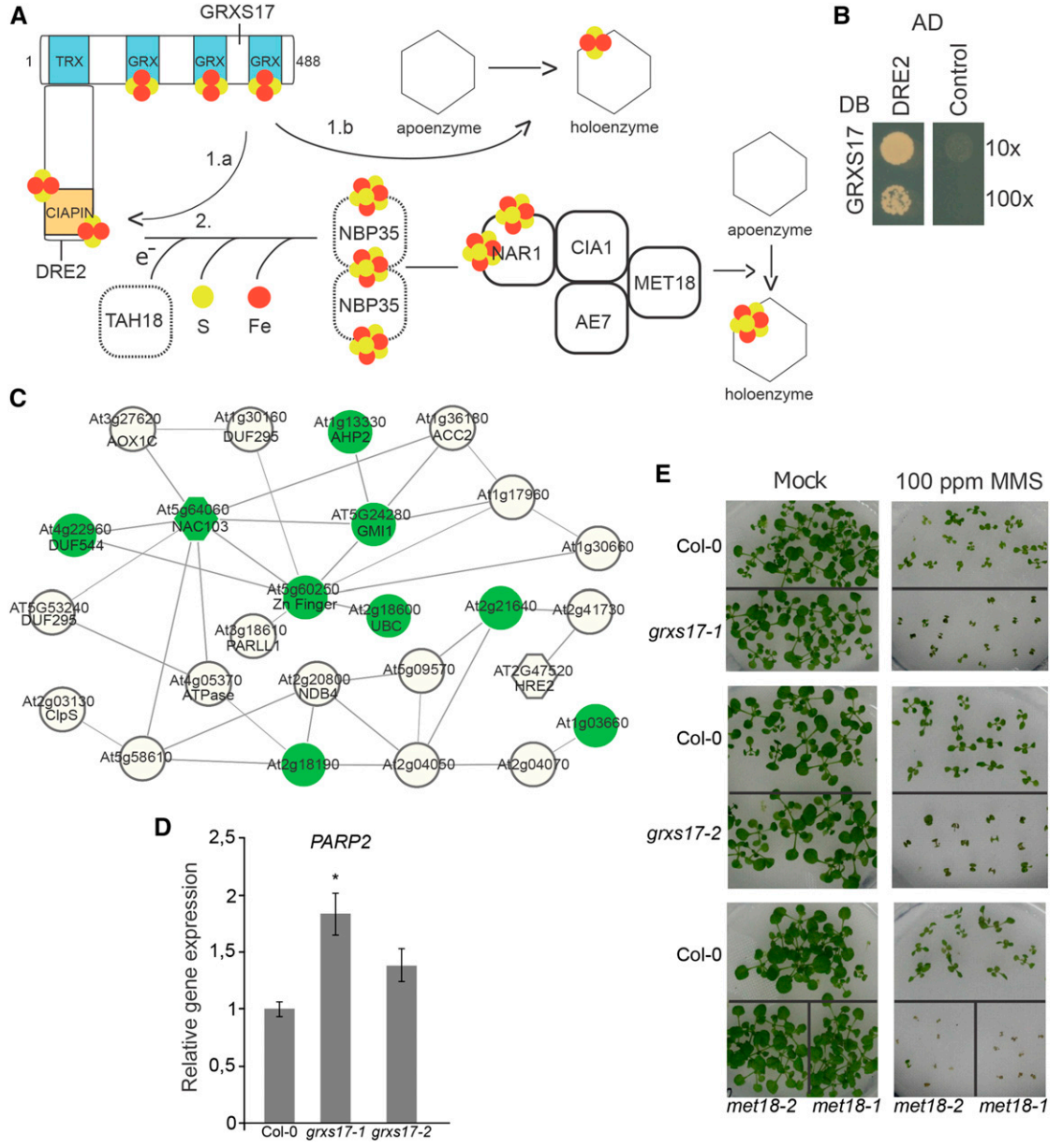

Figure 1. Loss-of-function *grxs17* plants display some degree of hypersensitivity to DNA damage. A, Hypothetical model of the CIA pathway and GRXS17 function. GRXS17 contains an N-terminal TRX domain and three GRX domains by which it interacts with three [2Fe-2S] clusters as a homodimer. GRXS17 also forms a complex with DRE2 that can bind two [2Fe-2S] clusters with its CYTOKINE INDUCED APOPTOSIS INHIBITOR1 (CIAPIN1) domain. GRXS17 can transfer a [2Fe-2S] cluster directly to DRE2 (1.a) or to a client apoprotein (1.b). DRE2 functions at the start of the CIA pathway in which a [2Fe-2S] matures to a [4Fe-4S] cluster (2) that can be delivered to client apoproteins. Full and dashed boxes indicate components that copurified or not with GRXS17 by TAP, respectively. B, GRXS17 directly interacts with DRE2. The PJ69-4A yeast strain was cotransformed with GRXS17 in pGBKT7gate and DRE2 in pGADT7gate. The 10× and 100× dilutions of transformed yeasts were dropped on selective medium lacking His. The empty pGADT7gate vector was used as control. One representative from three independent drops is shown. C, Coexpression network of up-regulated genes in *grxs17-1*. Nodes are genes that are significantly 2-fold up-regulated in *grxs17* seedlings; edges represent coexpression in ATTED-II (http://atted.jp/). Green nodes are also significantly and more than 2-fold induced upon genotoxic stress (bleomycin + mitomycin for 12 and 24 h). Hexagon nodes indicate putative transcription factors. D, Relative expression of the DNA-damage marker *PARP2* in 14-d-old Col-0, *grxs17-1*, and *grxs17-2* seedlings. Bars represent means ± SE of $n = 3$ (*$P < 0.05$, Student's *t* test). E, Hypersensitivity of *grxs17-1*, *grxs17-2*, *met18-1*, and *met18-2* to the DNA-damage agent MMS. Seedlings were grown for 17 d on 0.01% v/v MMS or in control conditions (mock).

interact with proteins related to different functions. It has recently been suggested that the human GRXS17 ortholog GRX3 establishes protein-protein interactions with its N-terminal TRX domain and that this interaction favors the correct orientation of the Fe-S cluster binding domains (GRX donors) to transfer the cluster to an acceptor protein (Banci et al., 2015).

The CIA pathway is responsible for providing Fe-S clusters to respective apoproteins in the cytosol and the nucleus (Bernard et al., 2013). In the current model, electrons provided by NADPH oxidation are transferred by Top1T722A MUTANT HYPERSENSITIVE and DEREPRESSED FOR RIBOSOMAL PROTEIN S14 EXPRESSION (DRE2) to the scaffold protein NUCLEOTIDE BINDING PROTEIN35. Once the [4Fe-4S] clusters have been assembled on the NUCLEOTIDE BINDING PROTEIN35 scaffold, they are transferred to target apoproteins by dedicated proteins forming the CIA targeting complex (Fig. 1A). In Arabidopsis, this complex is composed of NUCLEAR ARCHITECTURE RELATED1 (NAR1), CIA1, AS1/2 ENHANCER7 (AE7/CIA2), and METHIONINE REQUIRING18/METHYL METHANESULFONATE19 (MET18/MMS19) and locates to both the cytosol and the nucleus (Luo et al., 2012). Grx3, the yeast GRXS17 ortholog, has been demonstrated to interact with DRE2 in yeast (Zhang et al., 2011), and recently, it has been shown that the human GRX3 is able to transfer [2Fe-2S] clusters to anamorsin, the human DRE2 ortholog (Banci et al., 2015). We thus hypothesized that GRXS17 might similarly directly interact with DRE2 in Arabidopsis, which was confirmed by yeast two-hybrid analysis (Y2H; Fig. 1B). We confirmed this interaction in planta by bimolecular fluorescent complementation (BiFC). Proteins were fused with N-terminal or C-terminal fragments of GFP (designated nGFP and cGFP, respectively) and coexpressed transiently in leaves of *Nicotiana benthamiana* (Supplemental Fig. S1A). A cytosolic signal was obtained with the combination of nGFP-GRXS17 and DRE2-cGFP, which corresponded to the localization of GFP-DRE2 (Supplemental Fig. S1C). Thus, we concluded that Arabidopsis GRXS17 associates with the CIA complex as in yeast and humans.

Loss-of-Function *grxs17* Plants Show Some Degree of Hypersensitivity to DNA Damage

To obtain insights into the function of GRXS17, we profiled the transcriptome of *grxs17* loss-of-function seedlings. A transfer DNA (T-DNA) insertion line (*grxs17*-1; SALK_021301) described previously (Supplemental Fig. S1; Cheng et al., 2011; Knuesting et al., 2015) was characterized in detail and found to lack both *GRXS17* transcripts (Supplemental Fig. S2B) and GRXS17 protein (Supplemental Fig. S2C). Fourteen-day-old seedlings were grown in vitro and used for RNA sequencing

Table I. *GRXS17 associates with the CIA complex and Fe-S proteins in Arabidopsis cells and seedlings*

Proteins identified by mass spectrometry, with at least two significant peptides per identification and background subtracted (as described by Van Leene et al. [2015]). Numbers of independent TAP experiments in which the proteins were copurified with C terminally or N terminally TAP-tagged GRXS17 as bait in each system are presented. Interactions that were confirmed in yeast (Tarassov et al., 2008; Li et al., 2009; Zhang et al., 2011), in humans (Rual et al., 2005; Stehling et al., 2012, 2013; Rolland et al., 2014), or in Arabidopsis (this study; Arabidopsis Interactome Mapping, 2011; Couturier et al., 2014; Duan et al., 2015) are shown in bold. GSrh, GSrhino; Nd, Not determined; *, peptides retrieved cannot discriminate between CTU1 and CTU1L.

Name				No. of Affinity Purifications				
Arabidopsis	Locus	Orthologs		C-GSrh		N-GSrh		Total
		S. cerevisiae	*Homo sapiens*	Cells	Seedlings	Cells	Seedlings	
GRXS17	AT4G04950	Grx3/4	GRX3/GRLX3/PICOT	4	2	2	1	9
CIA pathways								
MET18	AT5G48120	Met-18/Mms19	**MMS19**	4	2	2	1	9
DRE2/CIAPIN	AT5G18400	**Dre2/Ciapin**	**Anamorsin/CIAPIN1**	4	2	2	–	8
NAR1	AT4G16440	Nar1	NARFL/IOP1	3	–	–	–	3
CIA1	AT2G26060	Cia1	**CIAO1**	2	–	–	–	2
AE7/CIA2	AT1G68310	Cia2	CIA2B/MIP18	2	–	–	–	2
Purine catabolism and salvage								
XDH1	AT4G34890	Nd	XDH/XOR/XO	3	2	1	–	6
URH1	AT2G36310	Urh1	Nd	–	2	–	1	3
URH2	AT1G05620	Urh1	Nd	–	2	–	1	3
UREG	AT2G34470	Not present	Not present	–	2	–	–	2
tRNA modification								
CTU1/ROL5	AT2G44270	Ncs6	CTU1	2*	–	1	–	1-3
CTU1L	AT1G76170	Ncs6	CTU12*		–		–	0-2
CTU2	AT4G35910	Ncs2	CTU2	1	–	1	–	2
Leu-tRNA ligase	AT1G09620	Cdc60	LARS	–	2	–	1	3
Other known Fe-S protein								
BolA2	AT5G09830	**Fra2**	BOLA2	–	3	–	–	3

(RNA-Seq). One hundred eighty-eight genes were found to be significantly up-regulated, and 209 were down-regulated (Supplemental Table S1). Using ATTED-II (http://atted.jp/), we identified a conserved coexpression network comprising 25 genes up-regulated in *grxs17-1* mutants (Fig. 1C; Supplemental Table S1). Many of the genes in this network are known to be induced upon genotoxic stress (Ascencio-Ibáñez et al., 2008). Because Arabidopsis mutant plants compromised in components of the purified CIA complex (Table I), namely AE7/CIA2 (Luo et al., 2012) and MET18/MMS19 (Han et al., 2015), have been reported to have increased expression of DNA-damage response genes (Luo et al., 2012; Han et al., 2015), we analyzed the expression of *POLY(ADP-RIBOSE) POLYMERASE2* (*PARP2*), a frequently used marker gene, in the *grxs17-1* mutant, as well as in an antisense line, denominated *grxs17-2*, that was previously described (Cheng et al., 2011) and which we confirmed to lack GRXS17 protein accumulation (Supplemental Fig. S2C). *PARP2* transcript levels were indeed induced in both mutant alleles (Fig. 1D). Therefore, we assessed the sensitivity of the *grxs17-1* and *grsx17-2* mutant lines to DNA-damage stress. In agreement with the transcriptome data, the *grxs17* mutants were found to display some degree of hypersensitivity to the DNA-damage agent MMS (Fig. 1E), though not as marked as the *met18* mutants (Fig. 1E; Luo et al., 2012; Han et al., 2015). Together, these data suggest that GRXS17 not only forms part of the CIA complex in Arabidopsis but also may contribute to its function in the DNA-damage response.

Metabolic Profiling of Loss-of-Function *grxs17* Plants Points to a Perturbed Flux through the Purine Salvage Pathway

Although human and yeast GRXS17 orthologs are essential for the maturation of cytosolic and nuclear Fe-S proteins (Mühlenhoff et al., 2010; Haunhorst et al., 2013), Arabidopsis GRXS17 has recently been shown to play only a minor role in maintaining the activity of two classes of cytosolic Fe-S enzymes (aconitases and aldehyde oxidases; Knuesting et al., 2015). Nonetheless, we identified another Fe-S enzyme, XDH1, to be associated with GRXS17 (Table I). XDH1 belongs to the family of xanthine oxidoreductases (XORs) that catalyze the oxidation of hypoxanthine and xanthine to uric acid during purine degradation. XDH1 is active as a homodimer in which each monomer has four cofactors: two [2Fe-2S] prosthetic groups, one FAD molecule, and one molybdenum cofactor (Moco), bound to the N-terminal, central, and C-terminal part of the protein, respectively (Zarepour et al., 2010).

Because XDH1 contains two [2Fe-2S] cofactors that are required for electron transfer to reduce the substrates xanthine and hypoxanthine (Zarepour et al., 2010), we investigated the GRXS17-XDH1 interaction in more detail. Interaction between XDH1 and GRXS17 was confirmed in a Y2H assay (Fig. 2A) and by BiFC, showing a cytosolic localization (Supplemental Fig. S1, B and C). To examine the physiological relevance of this interaction, we measured XDH activity in *grx17-1* and *grxs17-2* seedlings (Fig. 2B) but found no statistically significant difference in XDH activity compared with wild-type seedlings (Fig. 2B). Hence, similar to what was previously found for the enzymes cytosolic aconitase and aldehyde oxidase (Knuesting et al., 2015), our findings indicate that GRXS17 is not essential for XDH1 enzyme activity in plants.

In addition to XDH1, three additional proteins required for purine degradation were identified in complex with GRXS17: URIDINE RIBOHYDROLASE1 and

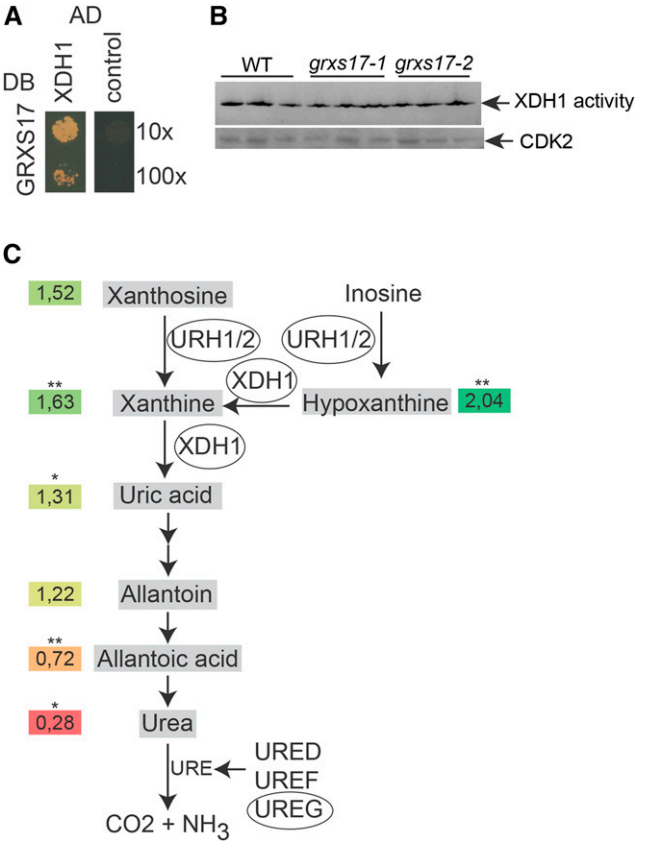

Figure 2. GRXS17 may contribute to the functioning of the purine salvage pathway. A, GRXS17 directly interacts with XDH1. The PJ69-4A yeast strain was cotransformed with GRXS17 in pGBKT7gate and XDH1 in pGADT7gate. The 10× and 100× dilutions of transformed yeasts were dropped on selective medium lacking His. The empty pGADT7-gate vector was used as control. One representative from three independent drops is shown. B, XDH1 activity measurements. One hundred micrograms of total protein extract obtained from the indicated plant lines was loaded in each lane (three biological repeats) of a native PAGE and subsequently stained using hypoxanthine as a substrate. C, Purine salvage pathway. Enzymes copurified with GRXS17 in the TAP analysis are encircled. Numbers are averaged relative abundances from five independent samples (*grxs17-1*/Col-0) of uric acid precursors and ureides mapped on the purine salvage pathway (*$P < 0.05$; **$P < 0.01$, Student's *t* test; colors: red, decreased; green, increased). The experiments were repeated twice with similar results. WT, Wild type.

2 (URH1/2) and the urease accessory protein UreG (Table I). URH1 and URH2 are nucleoside ribohydrolases with inosine and xanthosine hydrolytic activity, leading to hypoxanthine and xanthine generation (Riegler et al., 2011). Urease catalyzes the hydrolysis of urea to ammonia and carbon dioxide, which are the final products of purine degradation. In Arabidopsis, urease activation is mediated by the accessory proteins UreD, UreF, and UreG (Witte et al., 2005). To evaluate the impact of loss-of-function of *GRXS17* on purine metabolism, we measured the accumulation of uric acid precursors (hypoxanthine, xanthine, and xanthosine) and of ureides (uric acid, allantoin, allantoic acid, and urea) in wild-type and *grxs17* seedlings (Fig. 2C; Supplemental Fig. S3). Although the effects were modest, our results are in agreement with the function of XDH1 in the purine salvage pathway and point to a perturbed flux through this pathway in the *GRXS17* loss-of-function plants with enhanced accumulation of hypoxanthine, xanthine, and xanthosine and reduced accumulation of allantoic acid and urea. Together, these results suggest that association of GRXS17 with purine metabolism enzymes may be functionally relevant and may contribute to the purine salvage pathway.

GRXS17 Interacts with tRNA Thiolation Proteins

The TAP of GRXS17 protein complexes revealed interactions with several proteins that are linked to tRNA metabolism (Table I). For instance, we found GRXS17 to associate with the Arabidopsis orthologs of CTU1 and CTU2 required for 2-thiolation of U_{34} of the three cytosolic tRNA species tK(UUU), tE(UUC), and tQ(UUG). These tRNAs carry an $mcm^5s^2U_{34}$ modification, which is conserved throughout archae and eukaryotes (Fig. 3A; Leidel et al., 2009; Philipp et al., 2014). Although only the protein encoded by AT2G44270 was described as the Arabidopsis CTU1 ortholog (Leiber et al., 2010), several peptides copurified with GRXS17 could not be distinguished from the product of locus AT1G76170 with 93% sequence similarity to CTU1 (Table I) and was named CTU1-like (CTU1L). To verify the interaction between GRXS17 and CTU1 and CTU2, we performed Y2H and BiFC assays. Y2H indicated only a very weak interaction for both CTU1 and CTU2 (Fig. 3B). Through BiFC, we could confirm a cytosolic-localized GRXS17-CTU2 interaction (Fig. 3C; Supplemental Fig. S4), thus supporting the TAP results and confirming that GRXS17 interacts directly with CTU2. Interaction between GRXS17 and CTU1 could not be detected in BiFC, which may either be a false negative result or an indication of indirect interaction, for instance via heterodimerization with CTU2.

To further investigate the link between GRXS17 and CTUs, we tested if GRXS17 was required for tRNA thiolation in Arabidopsis. Thiolated tRNAs were visualized using their retardation in PAGE in the presence of [(*N*-acryloylamino)phenyl]mercuric chloride (APM), a compound that interacts with 2-thiouridine (Igloi, 1988). As reported previously, *ctu1* and *ctu2* T-DNA insertion lines did not contain thiolated tRNA (Fig. 3C; Leiber et al., 2010; Philipp et al., 2014). In contrast, in *grxs17-1* plants, levels of thiolated total tRNA were similar to wild type (Fig. 3C). Thus, GRXS17 interacts with CTU subunits but is not essential for their tRNA anticodon thiolation function in Arabidopsis.

GRXS17 and Elongator Functions Are Related in Arabidopsis

Whereas CTU1 and CTU2 are essential for 2-thiolation of mcm^5-modified tRNA anticodons, the ncm^5U_{34} modification itself is dependent on elongator (Fig. 3A; Huang et al., 2005; Selvadurai et al., 2014), a complex that is structurally and functionally conserved between *Saccharomyces cerevisiae* and Arabidopsis (Mehlgarten et al., 2010). ELO3, the Arabidopsis ortholog of yeast elongator subunit Elp3, contains histone acetyltransferase and radical sterile alpha motif domains, which were recently shown to be catalytically critical for the tRNA modification function of archaeal Elp3 (Selvadurai et al., 2014).

grxs17-1 and *grxs17-2* mutant plants exhibit an elongated leaf phenotype with larger leaf length/width ratio as compared to wild type (Supplemental Fig. S5, A and B), which is typical of elongator mutants (Nelissen et al., 2005). Therefore, we investigated the possibility of a link between GRXS17 and elongator. First, we studied the root and leaf phenotypes of *grxs17-1*, *grxs17-2*, and *elo3-6* in the Columbia-0 (Col-0) background. The *elo3-6* and the two *grxs17* mutant alleles had a reduced primary root growth (Fig. 4A), which was correlated with a reduced number of cortex cells in the root apical meristem (Fig. 4B), suggesting a faster transition to differentiation. Second, we measured the total leaf area in *elo3-6* and the two *grxs17* mutant alleles relative to wild-type plants. Notably, all three mutants had a similar growth profile: (1) larger juvenile leaves 1, 2, and 3, which are fully expanded at 24 d after germination (DAG); (2) a larger leaf 4, which is the transition to adult stage; and (3) smaller adult leaves 6, 7, and 8 because of a delay in growth in the mutants (Supplemental Fig. S5A). This is also reflected in the absence of leaf 8 and cauline leaves at the 24 DAG time point in some of the mutant genotypes (Fig. 4C). We examined the cellular basis of the changes in the fully developed leaf 3, of which the total cell number and final cell area are representative of cell proliferation and growth activities during its development. We observed that the cell area in all mutant lines was similar to that of the Col-0 control. However, the calculated number of cells per leaf was significantly higher in the two *grxs17* mutant genotypes and in the *elo3-6* line as compared to wild type (Supplemental Fig. S5, C and D), indicating that the larger leaf 3 area is the result of more cell proliferation in *grxs17* and *elo3-6* mutant lines.

Next, we compared our RNA-Seq dataset (Supplemental Table S1) with previously published microarray datasets of

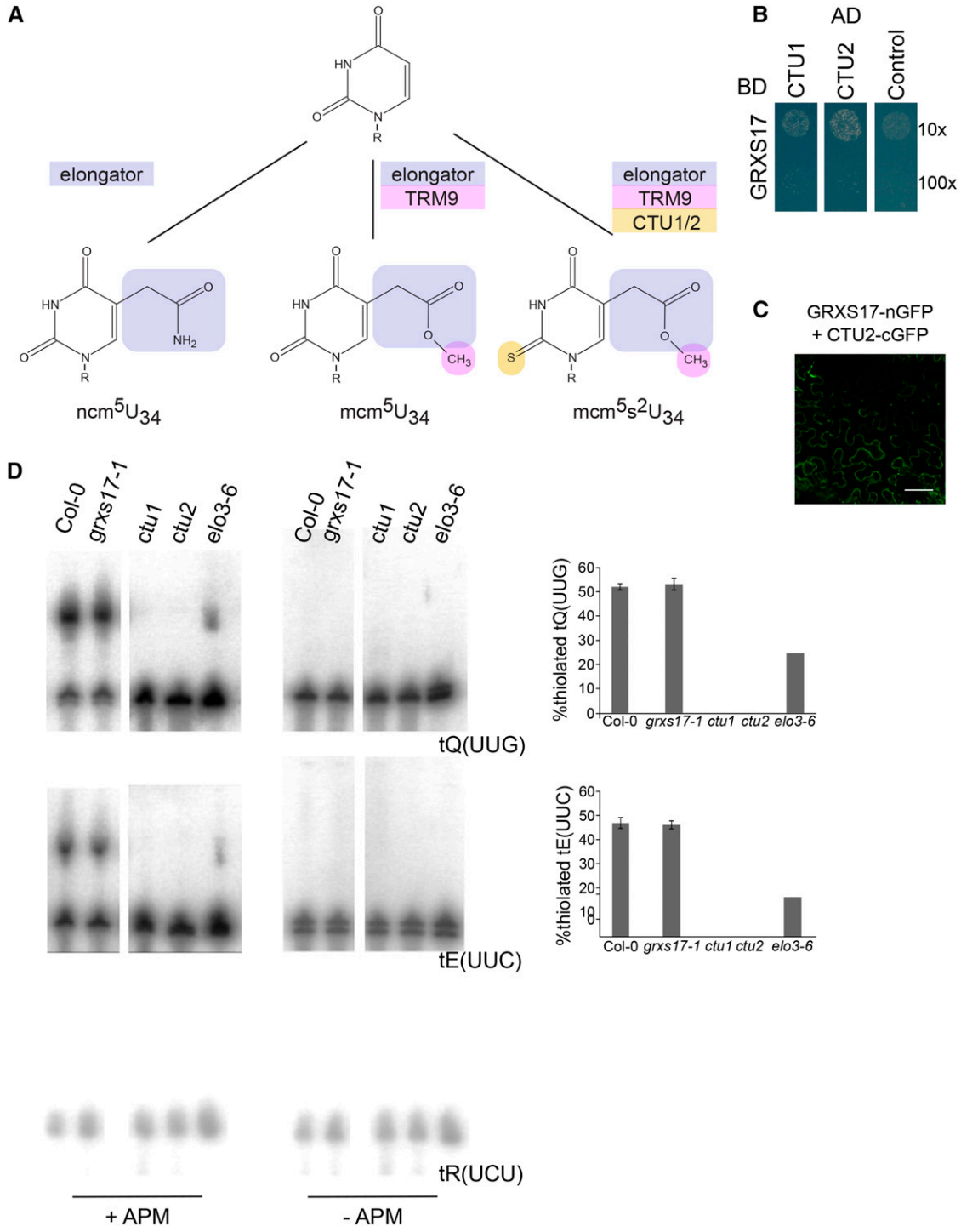

Figure 3. GRXS17 interacts with tRNA thiouridylases. A, Different types of tRNA modifications present in wobble uridines. Modifications by elongator, methylation by TRM9/12, and thiolation by CTUs are indicated in blue, pink, and yellow, respectively. R, Ribose. B, GRXS17 directly interacts with CTU1 and CTU2. The PJ69-4A yeast strain was cotransformed with GRXS17 in pGBKT7gate and CTU1 or CTU2 in pGADT7gate. The 10× and 100× dilutions of transformed yeasts were dropped on selective medium lacking His. The empty pGADT7gate vector was used as control. One representative from three independent drops is shown. C, GRXS17 interaction with CTU2 by BiFC. Fusion proteins with an N-terminal (nGFP) or C-terminal (cGFP) fragment of GFP were transiently coexpressed in *N. benthamiana* leaves and analyzed by confocal microscopy, 3 d after agro-infiltration. Negative controls are shown in Supplemental Figure S4. D, Total RNA extracted from Col-0, *grxs17-1*, *ctu1*, *ctu2*, or *elo3-6* was separated using PAGE in the presence or absence of APM. Subsequently, RNA blots were probed against tQ(UUG), tE(UUC), or control tR(UCU). Quantification of thiolated modified tRNAs (right panels). Bars represent means ± SD of three biological independent samples. No statistical significances were detected between Col-0 and *grxs17-1*.

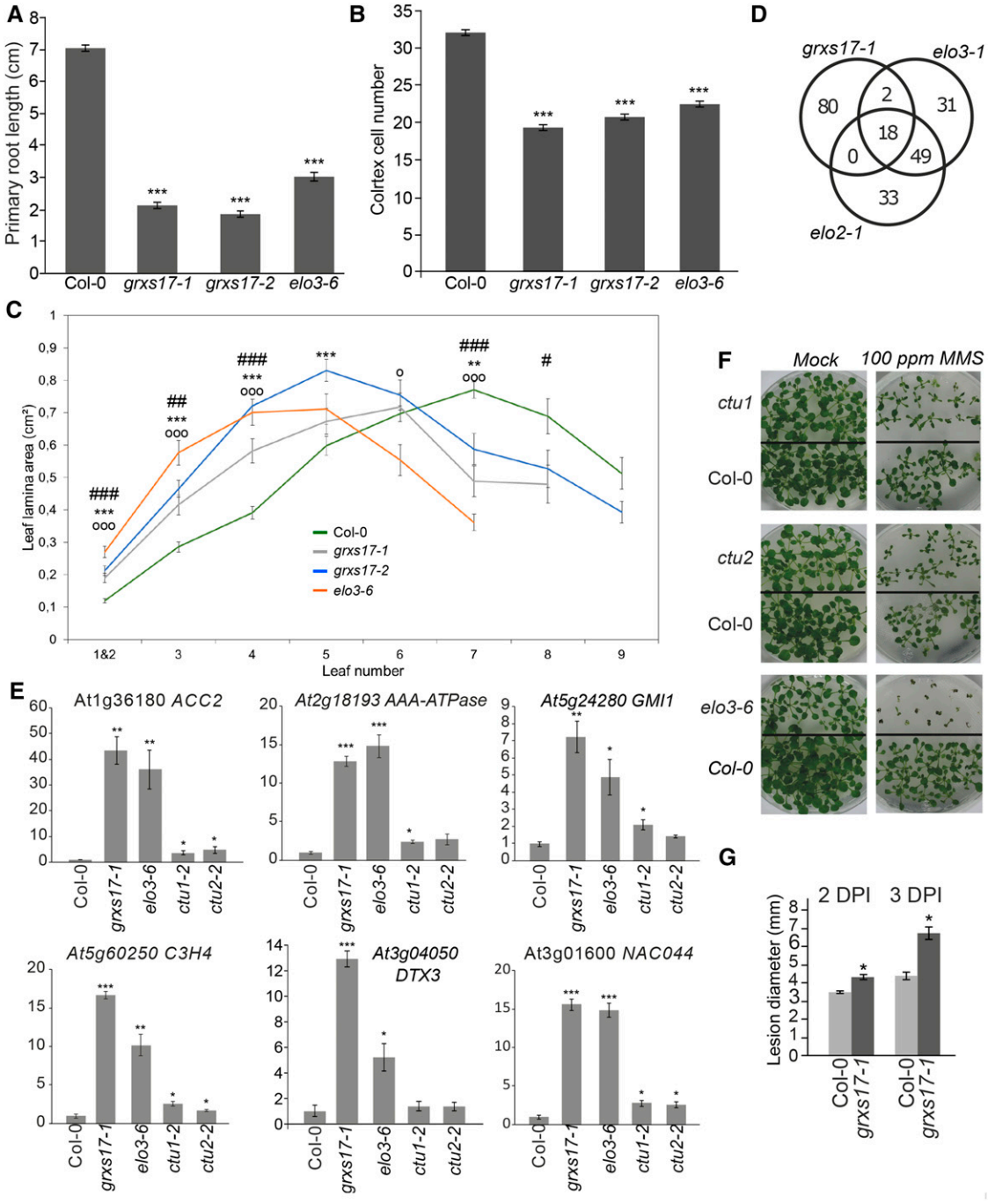

Figure 4. *grxs17* and *elo3-6* mutants show similar physiological and molecular defects. A–C, Analysis of root and leaf growth. A, Primary root length of 11-d-old Col-0, *grxs17-1*, *grxs17-2*, and *elo3-6* seedlings grown on Murashige and Skoog ($n > 21$). B, Number of cortex cells in the root apical meristem of seedlings 5 DAG ($n > 34$). C, Lamina area of leaf series of 24-d-old plants germinated in soil ($n > 10$) Bars represent means ± SE (*$P < 0.05$; **$P < 0.01$; ***$P < 0.001$, Student's *t* test, # comparison between Col-0 and *grxs17-1*, * for Col-0 and *grxs17-2*, and ° for Col-0 and *elo3-6*). D and E, Transcriptome analysis. D, Overlap between the top 100 genes up-regulated in *grxs17-1* for which a probeset is present on the ATH1 microarray and the top 100 probesets significantly up-regulated in *elo2-1* and *elo3-1*. E, qPCR validation of gene expression in *grxs17-1*, *elo3-6*, *ctu1-2*, and *ctu2-2* mutants. The expression ratio relative to that in wild-type Col-0 seedlings is plotted (set at 1). Bars represent means ± SE of $n = 3$ (*$P < 0.05$; **$P < 0.01$; ***$P < 0.001$, Student's *t* test). F, Hypersensitivity of *ctu1*, *ctu2*, and *elo3-6* to MMS. Seedlings were grown for 17 d on 0.01% v/v MMS or under control conditions (mock). G, Hypersensitivity of *grxs17-1* mutants to the necrotrophic pathogen *B. cinerea*. Lesion diameter in *grxs17-1* and Col-0 plants infected with *B. cinerea*, 2 and 3 d postinoculation. Bars represent means ± SE with $n = 32$ (*$P < 0.05$, Student's *t* test).

the elongator mutants *elo2-1* and *elo3-1* (Nelissen et al., 2005). Although the latter dataset was performed on mutants in the Landsberg *erecta* ecotype and with a different experimental setup, we observed a large overlap between the top 100 genes induced in *grxs17-1*, *elo2-1*, and *elo3-1* (Fig. 4D). The overlap comprised the DNA-damage network indicated above (Fig. 1C). Indeed, loss of *ELO3* has been reported to lead to a DNA-damage response (Xu et al., 2012). We assessed this observation further by analyzing gene expression in the *grxs17* and *elo3-6* mutants and in the T-DNA insertion lines of *CTU1* and *CTU2*, called *ctu1* and *ctu2*, all in the Col-0 background (Fig. 4E; Supplemental Fig. S6). Indeed, all genes tested that were up-regulated in *grxs17* mutants were also up-regulated in *elo3-6*. Similarly, also in *ctu1* and *ctu2* we observed an upregulation of many *grxs17*-up-regulated genes, although more modest. In agreement with these results, *ctu1* and *ctu2* also showed some degree of sensitivity to the DNA-damage agent MMS (Fig. 4F).

Finally, previous reports indicated that the elongator subunits ELP2 and ELP3/ELO3 are involved in the salicylic acid signaling pathway (DeFraia et al., 2010, 2013) and that the elongator complex is required for Arabidopsis resistance to necrotrophic fungal pathogens such as *Botrytis cinerea* and *Alternaria brassicicola* (Wang et al., 2015). Therefore, we tested the susceptibility of the *grxs17-1* mutant to *B. cinerea*. Compared with wild-type plants, *grxs17-1* plants were more susceptible to *B. cinerea* infection (Fig. 4G), suggesting that GRXS17 plays a role in the defense response against *B. cinerea*.

Taken together, our data indicate that *grxs17* and *elo3* mutants have similar phenotypes at the molecular, cellular, and physiological level, both in growth and in defense, and thus support a joined, but not necessarily identical, role in the functioning of particular processes such as tRNA modification.

GRX and Elongator Functions Are Related, Also in Yeast

Given the conservation of the GRX proteins in eukaryotes, we wanted to test whether the yeast orthologs of Arabidopsis GRXS17, i.e. Grx3/4 (Herrero and de la Torre-Ruiz, 2007), also have similar related functions in tRNA modification by elongator in *S. cerevisiae*. Because *grx3 grx4* double mutants are barely viable in S288c (Wu et al., 2012) and lethal in the background of yeast strain W303-1A, we used a previously described *GRX3* deletion strain of W303 that maintains the *GRX4* gene under the control of a *GAL1* promoter, which is repressible by Glc and inducible by Gal (Mühlenhoff et al., 2010). W303 contains an ochre stop codon (UAA) mutation in the ADE2 locus (*ade2-1*ochre), which leads to premature translation termination and causes adenine auxotrophy (Fig. 5A). This phenotype can be suppressed by read-through of *SUP4*, an ochre suppressor $tRNA^{Tyr}$ carrying a U_{34} mutation in its anticodon (Goodman et al., 1977; Huang et al., 2005; Jablonowski et al., 2006; Fig. 5A). Because the *SUP4* $tRNA^{Tyr}$ needs an mcm^5-modified U_{34} to decode the UAA triplet as Tyr (Huang et al., 2005; Jablonowski et al., 2006), it cannot suppress the *ade2-1*ochre reporter without proper mcm^5 formation at U_{34}. *SUP4* failed to promote stop codon read-through of *ade2-1*^{ochre} and hence, conferred adenine auxotrophy in the yeast reporter strain lacking *GRX3* function, even if *GRX4* was not repressed (Fig. 5A). This indicates that *GRX3* gene function in yeast is critical for *SUP4* function and thus supports a related role with elongator, as in Arabidopsis.

When we analyzed tRNA thiolation in *elo3-6* mutant, we observed, in contrast to *grxs17-1*, almost no thiolated tRNA (Fig. 3D). These results suggest that *grxs17-1* presents no strong defect in mcm^5 modification in plants based on the absence of a strong thiolation defect. However, in yeast and plants, the GRXs Grx3/4

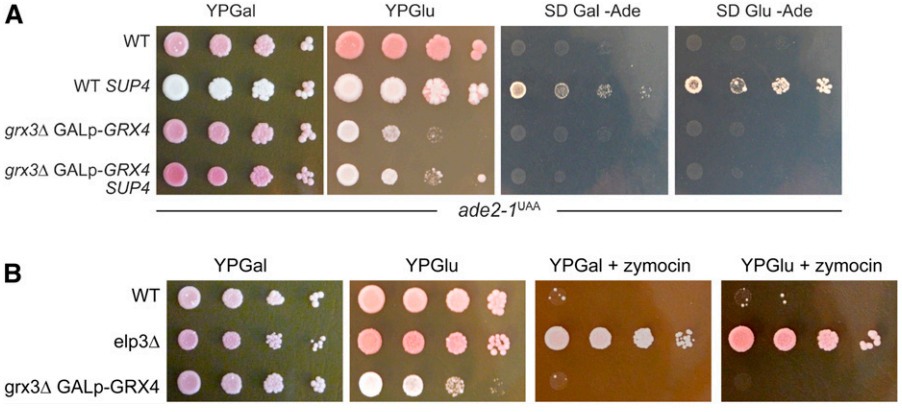

Figure 5. GRX and elongator function are related in yeast. A, GRX3 is required for *SUP4* suppressor tRNA function in yeast. Serial 10-fold cell dilutions of wild-type (WT) yeast strain W303-1A (*ade2-1*^{UAA}) and its derivative *grx3Δ GALp-GRX4* (Mühlenhoff et al., 2010) both either lacking or carrying the *SUP4* ochre tRNA suppressor were grown on rich (YP) medium containing Gal or Glc (Glu) to repress or induce *GRX4* expression, respectively. In addition, the indicated yeast strains were cultivated on minimal (SD) medium containing Gal or Glu but lacking Ade to probe for SUP4-mediated adenine prototrophy. B, Same strains as in (A) and including *elp3Δ* were grown in the presence or absence of zymocin. Both experiments were repeated with similar results.

and GRXS17 may have a potential influence on elongator tRNA modification function, which we have previously shown to be conserved in and functionally exchangeable between *S. cerevisiae* and Arabidopsis (Mehlgarten et al., 2010). In the light of these findings, it is interesting to note that the *GRX3* gene was identified previously as a high-copy suppressor in yeast of growth inhibition by zymocin, a fungal tRNase ribotoxin complex (Jablonowski et al., 2001; Jablonowski and Schaffrath, 2007). Zymocin activity targets elongator-dependent mcm^5s^2U34 modifications in tRNA anticodons (Lu et al., 2005; Jablonowski et al., 2006) and eventually kills *S. cerevisiae* cells. Therefore, loss of tRNA modification in elongator (*elp*) or tRNA methyltransferase (*trm9*) mutants protects against zymocin, making the tRNase a useful tool for diagnosing elongator function and, hence, tRNA modification in yeast (Nandakumar et al., 2008) and potentially in Arabidopsis (Mehlgarten et al., 2010; Leitner et al., 2015). We tested zymocin resistance in a yeast *ELP3* deletion strain and in a *GRX3* deletion strain having the *GRX4* gene under control of the *GAL1* promoter. As expected, deletion of *ELP3* resulted in resistance to zymocin due to loss of $mcm^5s^2U_{34}$ modification (Fig. 5B). However, when *GRX3/4* were deleted, yeast cells could not grow in the presence of the toxin. Although these results suggest appropriate tRNA modifications, our *SUP4* assay above (Fig. 5A) together with previous data showing that high-copy *GRX3* confers zymocin resistance (Jablonowski et al., 2001), may indicate that the absence of *GRX3/4* function differentially affects mcm^5 or mcm^5s^2 modifications at U_{34}, an option that has to await further elucidation.

DISCUSSION

Cytosolic monothiol GRXs are required in Fe-S cluster delivery in yeast and mammals. In plants, it remained unclear whether they have similar functions. Here, we used interactome analysis and in-depth functional characterization of a loss-of-function mutant to establish that that the sole class II cytosolic monothiol GRX from Arabidopsis associates with CIA components and Fe-S client proteins and contributes to their functioning.

Profiling of Loss-of-Function *grxs17* Plants Points to an Elevated DNA-Damage Response

The function of many CIA components in yeast, mammals, and Arabidopsis has been associated with genomic stability, DNA repair, and metabolism, because many proteins necessary for DNA replication and repair are known to contain Fe-S clusters. In yeast and humans, Met-18/MMS19 has been shown to associate not only with several other CIA components, but also with Fe-S target proteins involved in DNA metabolism and to mediate the maturation of certain Fe-S proteins involved in DNA repair and replication (DNA helicases, polymerases, nucleases or glycosylases; Gari et al., 2012; Stehling et al., 2012; van Wietmarschen et al., 2012). The human MMS19 has been shown to be necessary for the maturation of only certain Fe-S proteins, mostly involved in DNA metabolism, but not for the activity of cytosolic aconitase iron regulated protein1 (IRP1) or Gln phosphoribosylpyrophosphate amidotransferase (Stehling et al., 2012). Human GRX3 is able to bind, in addition to [2Fe-2S] clusters, [4Fe-4S] clusters in vitro, which is necessary for the maturation of apo-IRP1 into aconitase (Xia et al., 2015), thus suggesting that GRX3/GRXS17, and not MMS19/MET18, is involved in the transfer of [4Fe-4S] clusters necessary for IRP1 maturation. This hypothesis is in accordance with the decrease in cytosolic aconitase activity observed in the Arabidopsis *grxs17-1* mutant (Knuesting et al., 2015).

In Arabidopsis, MET18 also interacts with DNA polymerases and facilitates the maturation of Fe-S clusters on DNA polymerases in the cytosol (Han et al., 2015). Another MET18-interacting protein is the DNA demethylase ROS1, an Fe-S client protein that requires the Fe-S cluster for its activity, linking the CIA pathway with epigenetic modifications (Duan et al., 2015). Accordingly, an elevated DNA-damage response was found in Arabidopsis mutants deficient in CIA complex components, such as *ae-7* and *met18* (Luo et al., 2012; Han et al., 2015), or in Fe-S cluster containing proteins, such as *elo3* (Xu et al., 2012).

In our study, we discovered a network (or regulon) that comprises genes involved in the genotoxic (DNA-damage) stress response to be up-regulated in the *grxs17-1* mutant. Accordingly, we found that *grxs17* plants present some degree of hypersensitivity to the DNA-alkylating agent MMS. A similar response has previously been reported for the *ae-7*, *met18*, and *elo3-6* mutants (Luo et al., 2012; Xu et al., 2012; Han et al., 2015). Given that most enzymes implicated in DNA replication and DNA repair contain Fe-S clusters, our data suggest that GRXS17 and its association with the CIA complex may be necessary for their correct functioning and thus in genome integrity maintenance in plants.

GRXS17 Associates with Fe-S Client Proteins

Among the GRXS17-associated proteins that we identified by TAP were CTU1 and CTU2, two proteins essential for the thiolation of uridine at the wobble position of cytosolic tRNA in eukaryotes (Björk et al., 2007; Schlieker et al., 2008; Leidel et al., 2009). CTU1 presents homology with *Escherichia coli* TtcA, the protein responsible for the thioltransferase activity necessary for s^2C_{32} tRNA thiolation, a tRNA modification not present in eukaryotes (Jäger et al., 2004). *E. coli* TtcA was shown to bind, through three conserved Cys residues, Fe-S clusters that are essential for its activity (Bouvier et al., 2014). The conserved motifs Cys-X_1-X_2-Cys present in *E. coli* TtcA and Arabidopsis CTU1 suggest that Arabidopsis CTU1(L) proteins could be Fe-S client proteins. Accordingly, proteins from the CIA

machinery are known to be required for 2-thio modification of cytosolic tRNAs, suggesting that at least one cytosolic or nuclear protein containing Fe-S clusters is necessary for thiolation of cytosolic tRNAs (Nakai et al., 2007). Accordingly, GRXS17 could be involved in the transfer of putative Fe-S clusters to a CTU1(L)/CTU2 complex.

Several proteins already known to bind Fe-S clusters were also found in our GRXS17 TAP interactome, including BolA2 and XDH1. Interactions between GRX and BolA proteins are conserved in yeast, humans, and plants. In all of these eukaryotes, it has been demonstrated that the GRX and BolA domains are bridged by the binding of a [2Fe-2S] cluster (Li et al., 2009, 2012; Couturier et al., 2014). However, GRXS17 can also bind Fe-S clusters independently of BolA2 interaction, through the formation of Fe-S bridged homodimers, and it can contribute to the activity of cytosolic Fe-S enzymes (Knuesting et al., 2015).

In yeast, Grx3/4 are localized in the nucleus, where they regulate the nuclear export of Aft1, a transcription factor that regulates Fe-responsive gene expression under low Fe conditions (Pujol-Carrion et al., 2006). Heterodimerization of Grx3/4 with the BolA-like protein Fra2 leads to nuclear export of Aft1 (Pujol-Carrion et al., 2006; Li et al., 2009). In both yeast and humans, GRXs play an important role in Fe utilization. Grx3/4-deficient yeast cells have defects in de novo synthesis of Fe-S clusters and heme, two of the major Fe-consuming processes in these organisms. The Fe content is not decreased in these yeast cells, but the Fe is not bioavailable due to deficient Fe delivery to mitochondria. A similar defect in Fe bioavailability was observed in zebrafish (*Danio rerio*) and HeLa cells when HsGRX3 (or the zebrafish ortholog) was depleted (Mühlenhoff et al., 2010; Haunhorst et al., 2013). In plants, BolA2 does not seem to play a role in Fe homeostasis, and the biological output of the GRXS17-BolA2 interaction remains an unanswered question (Couturier et al., 2014; Roret et al., 2014).

XDH1, in turn, belongs to the family of XORs and is a central player in purine catabolism. In Arabidopsis, two XOR-encoding genes are present with a strict XDH activity, i.e. *XDH1* and *XDH2*. Although both genes are located close to each other on the same chromosome, *XDH2* is expressed constitutively at basal levels, whereas *XDH1* is differentially expressed upon several developmental and environmental stimuli (Hesberg et al., 2004). Plants deficient in XDH1 are affected in growth and development. Seedlings with RNAi-mediated silencing of *XDH1* are smaller than wild-type plants with shorter flowering stems, smaller fruit size, and higher sterility rate (Nakagawa et al., 2007). In addition, XDH1-deficient plants also show earlier onset of age-dependent, dark-induced leaf senescence (Nakagawa et al., 2007; Brychkova et al., 2008) and decreased tolerance to drought stress (Watanabe et al., 2010). In accordance with the function of XDH1 in purine catabolism, precursors of uric acid (hypoxanthine and xanthine) are significantly more abundant in XDH1-deficient plants, whereas downstream products (allantoic acid and urea) are less abundant (Nakagawa et al., 2007; Brychkova et al., 2008). Quantification of these metabolites in *grxs17-1* plants indicated that these purine catabolism intermediates also accumulate differentially in the absence of *GRXS17*, reflecting a perturbed flux through the purine salvage pathway. However, it is interesting to note that despite the apparent clarity of these results, certain aspects of the changes in the levels of these metabolites were unexpected, namely the 20% increase in uric acid in the mutant in spite of the reduction of the activity of XDH1. The most likely explanation for this is the upregulation of another, as-yet-undefined, route of uric acid production in an unsuccessful (when viewed from the standpoint of the other downstream metabolites) attempt to compensate for the deficit of XDH1. This aspect suggests additional complexity in the regulation of this pathway and thus warrants further experimental study.

Remarkably, no overlap was found between the interacting partners identified in our study and those in a recent study in which affinity chromatography with HIS-tagged GRXS17 was used to identify GRXS17-interacting proteins (Knuesting et al., 2015). Interactors reported in the latter study were more related to signaling and included the transcriptional regulator Nuclear Factor Y Subunit C11/Negative Cofactor 2α (Knuesting et al., 2015). The discrepancy between these two interactomes could be due to differences in technical procedures and suggests that GRXS17 is able to interact with even more proteins than reported here and that it may be involved in different cellular processes.

GRXS17 Function Is Evolutionarily Conserved

The evolutionary conservation of the processes described in this paper is strong: CIA complex, GRX, XOR, and tRNA-modifying proteins are all conserved in plants and humans. Fe-S proteins are thought to be reminiscent of the origin of life, when Fe and S were readily available under a reducing, anaerobic environment. Metabolic pathways that evolved at these early stages of life became essential to all living organisms, and many of them require Fe-S proteins (Sheftel et al., 2010). Because Arabidopsis *grxs17* seedlings actually only show mild developmental defects (Cheng et al., 2011; Knuesting et al., 2015) in contrast to the strong developmental defects associated with GRX depletion in yeast or animal cells, plants such as Arabidopsis may have evolved alternative protein(s) or pathway(s) that can take over these evolutionary conserved tasks.

The role of GRX proteins in the CIA pathway is still not entirely understood. In yeast, incorporation of Fe-S clusters into both cytosolic and mitochondrial proteins is dependent on Grx3/4 (Mühlenhoff et al., 2010). We establish here that, in plants, GRXS17 associates with several components of the CIA complex, including DRE2, NAR1, CIA1, AE7/CIA2, and MET18. GRXS17-DRE2 interaction is conserved in yeast and humans, in which the orthologs also interact directly and in which

this close interaction allows the transfer of the [2Fe-2S] clusters from the GRX to DRE2 (Banci et al., 2015; Fig. 1A). In humans, disturbance of the DRE2/Anamorsin-GRX interaction has been proposed as a strategy to reduce cell proliferation in solid tumors in which *Anamorsin* expression is enhanced (Saito et al., 2011). Possibly, because maturation of DRE2 in humans is dependent on GRX3, GRX3 might, analogously to GRXS17, form the bridge between the mitochondrial and cytosolic Fe-S assembly machineries by providing the initial Fe-S cluster to the essential CIA proteins. Alternatively, GRXS17 might specifically contribute to the maturation of [2Fe-2S] cluster-containing proteins in the cytosol and the nucleus, because the clusters assembled by the CIA are of the [4Fe-4S] type. GRXS17 might thus associate with the CIA-targeting complex and function as a [2Fe-2S] specific adaptor for this complex.

MATERIALS AND METHODS

Plant Material and Growth Conditions

All mutant lines used in this study were in the Col-0 ecotype background. *grxs17-1* (SALK_021301), *grxs17-2* (antisense line), *rol5-2/ctu1-2* (GK-709D04), *ctu2-2* (GK-686B10), *elo3-6* (GK-555H06), *met18-1* (SALK_121963), and *met18-2* (SALK_147068) mutants were described previously (Leiber et al., 2010; Nelissen et al., 2010; Chen et al., 2011; Luo et al., 2012; Philipp et al., 2014). Arabidopsis (*Arabidopsis thaliana*) seeds were sterilized by the chlorine gas method and sown on sterile plates containing Murashige and Skoog medium supplemented with 1% (w/v) Suc, 0.8% (w/v) agarose, pH 5.7. Plates were kept 2 d in the dark for stratification at 4°C before being transferred to a growth room at 21°C with a 16-h light/8-h dark regime, with a light intensity of 80 μmol m^{-2} s^{-1}, unless mentioned otherwise.

Cloning and Site-Directed Mutagenesis

The coding sequence of *GRXS17*, *DRE2*, *CTU1*, and *CTU2* were amplified from cDNA obtained from wild-type Arabidopsis Col-0 seedlings, using specific primers (Supplemental Table S3) containing Gateway recombination attB sites. The amplified ORFs were then recombined with pDONR207 and transferred to the corresponding pDEST Gateway vectors.

Yeast Strains, Media, and SUP4 tRNA Suppressor Assay

Y2H analysis was performed as described previously (Cuéllar Pérez et al., 2013). In brief, the *Saccharomyces cerevisiae* PJ69-4A strain was cotransformed with pGADT7 and pGBKT7 vectors containing bait and prey, respectively. Transformants were selected on synthetic defined (SD) medium lacking Leu and Trp. Three individual transformants were grown overnight in liquid medium lacking Leu and Trp, and a 10-fold dilution of these cultures was dropped on control and selective solid media additionally lacking His. Empty vectors were used as negative controls and yeast cells were allowed to grow for 2 d at 30°C before interaction was scored.

For the conventional SUP4 tRNA suppressor assay based on *ade2-1* ochre read-through (Huang et al., 2005), we used W303-1A strain (*MATa ura3-1, ade2-1, trp1-1, his3-11, 15, leu2-3,112*; Mortimer and Johnston, 1986) and its p*GAL*-GRX4/grx3Δ derivative (W303-1A but pGRX4::*GAL-L-natNT2*; grx3Δ::*LEU2*; Mühlenhoff et al., 2010). Routine yeast growth was performed in rich yeast extract, peptone dextrose (YPD), or Gal (YPG) media or on SD medium containing 2% (w/v) dextrose (SD Glu) or 2% (w/v) Gal (SD Gal; Sherman, 2002). Both lacked adenine to check for *ade2-1 ochre* read-through by the tRNA suppressor SUP4 and formation of adenine prototrophic cells (Jablonowski et al., 2006). The latter involved growth for 3 d at 30°C of 10-fold serial dilutions of yeast strains W303-1A and p*GAL*-GRX4/grx3Δ transformed with SUP4 on a single-copy plasmid pTC3 (Shaw and Olson, 1984; Jablonowski et al., 2009).

TAP

N or C terminally tagged TAP constructs (GS or GSrh tag) were generated as described previously (Van Leene et al., 2015). They were used for the transformation of Arabidopsis PSB-D cell suspension cultures without callus selection and further grown and subcultured as described by Van Leene et al. (2011). Stably transformed cultures were scaled up and harvested 6 d after subculturing. Transgenic Arabidopsis seeds were generated by floral dip (Clough and Bent, 1998), using Col-0 as the background ecotype and the same constructs as for cell culture transformation. Transformants were selected, and purifications were performed as described by Van Leene et al. (2015), with the exception that no benzonase treatment was performed on the cell culture extracts. Expression of TAP-tagged constructs was verified on an aliquot of total protein extract before purification.

BiFC

pCaMV35S:ORF-tag constructs using the N- or C-terminal part of GFP (nGFP and cGFP, respectively) were constructed by triple Gateway reactions using pK7m34GW or pH7m34GW (Karimi et al., 2005) as described previously (Boruc et al., 2010). pCaMV35S::tag-ORF constructs were generated by double Gateway recombination using pH7m24GW2 or pK7m24GW2 (Boruc et al., 2010). The constructs were coexpressed together with a *P19*-expressing *Agrobacterium tumefaciens* strain (Voinnet et al., 2003) in *Nicotiana benthamiana* using *Agrobacterium*-mediated transient transformation with a modified infiltration buffer (10 mM $MgCl_2$, 10 mM MES, pH 5.7, 100 μM acetosyringone). Interactions were scored by screening the lower epidermal cells for fluorescence using LEICA SP2 confocal microscopy, 3 d after transformation.

RNA-Seq

Seedlings were grown in vertical plates in three biological repeats for 14 d in Murashige and Skoog medium supplemented with 1% (w/v) Suc. Seedlings were frozen in liquid nitrogen, and total RNA was extracted using the RNeasy plant mini kit (Qiagen) and DNase I (Promega) treatment. A Trueseq RNA-Seq library (Illumina) was compiled and sequenced as 50-bp single read using the Illumina HiSEquation 2000 technology at GATC Biotech. Read quality control, filtering, mapping to The Arabidopsis Information Resource 10 version of the Arabidopsis genome, and read counting were carried out using the Galaxy portal running on an internal server (http://galaxyproject.org/). Sequences were filtered and trimmed with the Filter FASTQ v1 and FASTQ Quality Trimmer v1 tools, respectively, with default settings (http://www.bioinformatics.babraham.ac.uk/projects/fastqc/). Reads were subsequently mapped to The Arabidopsis Information Resource 10 version of the Arabidopsis genome using GSNAPv2 (Wu and Nacu, 2010), allowing a maximum of five mismatches. The concordantly paired reads that uniquely map to the genome were used for quantification on the gene level with HTSeq-count from the HTSeq python package (Anders et al., 2015). Data were normalized using TMM, implemented in edgeR (Robinson et al., 2010), and common dispersion was then estimated using the conditional maximum likelihood method (Robinson and Smyth, 2008). Differentially expressed genes were defined by a 2-fold difference between mutant lines and the wild-type control with P-value < 0.05. The false discovery rate was limited to 5% according to Benjamini and Hochberg (1995).

Gene Expression Analysis

Seedlings were grown in the same conditions described for RNA-Seq, and total RNA was isolated as mentioned above. One microgram of RNA was used for cDNA synthesis using the iScript kit (Bio-Rad). Quantitative reverse transcriptase-PCR was performed on a LightCycler 480 system (Roche) using the Fast Start SYBR Green I PCR mix (Roche). At least three biological repeats and two technical repeats were used for each analysis. Data were analyzed using the second derivative maximum method, and relative expression levels were determined using the comparative cycle threshold method. Primer sequences are provided in Supplemental Table S3.

tRNA Extraction and Analysis

Seedlings were grown for 14 d in half-strength liquid Murashige and Skoog medium supplemented with 1% (w/v) Suc and 100 mg/L myoinositol. Seedlings were frozen in liquid nitrogen, and total RNA was extracted according to Björk et al. (2001). One-half microgram of total RNA was resolved on 8%

acrylamide gels containing 0.5× TBE, 7 M urea, and 50 μg/mL APM. Northern-blot analysis was performed essentially as described in Leidel et al. (2009), with the following probes: 5′-TGGCGCCGTCTGTGGGGATCG-3′ to detect tK(UUU), 5′-TGGAGGTTCTACCGGGAGTCGAACC-3′ to detect tQ(UUG), 5′-TGGCTCCATTGCCGGGAATCGAACC-3′ to detect tE(UUC) and as negative control for nonthiolated tRNAs, 5′-TGGCACACCCGGTGGGACTCG-3′ to detect tR(UCU), and 5′-TGGTGCGTCTGCCGGGAGTCG-3′ to detect tG(UCC).

Immunoblot Analysis

After quantification of the protein content as described by Bradford (1976), the indicated protein samples were loaded on a 4% to 15% TGX gel (Bio-Rad) and ran for 20 min at 300 V. Next, proteins were transferred to 0.2-μm polyvinylidene difluoride membranes (Bio-Rad) with the Transblot Turbo (Bio-Rad). Chemiluminescent detection was performed with western Bright ECL (Isogen).

Anti-GRXS17 Antibody

GRXS17 was cloned into the pDEST17 vector (Invitrogen) and expressed in the *Escherichia coli* BL21(DE3) strain. The 6xHIS-GRX17 recombinant protein was purified by IMAC using Ni-NTA (Qiagen) resin followed by size exclusion chromatography using an Äkta purifier equipped with a Superdex200 column (GE Healthcare). A rabbit was immunized with the purified recombinant 6xHIS-GRX17 in the service facilities of Agro-Bio (France). Total serum was collected 63 d postimmunization. A 1/5,000 dilution of this antibody and a 1/10,000 dilution of anti-rabbit IgG-HRP (GE) were used for immunoblotting.

DNA-Damage Agent

Sterilized seeds were geminated in Murashige and Skoog medium, transferred after 4 d to Murashige and Skoog plates supplemented or not with 0.01% v/v MMS (Sigma) and scored after 17 d. The experiment was performed in triplicate.

Root Phenotype Analysis

Seedlings grown vertically at 21°C under 24-h light conditions (75 μmol m^{-2} s^{-1}) were used for root analysis. The root meristem size was determined 5 DAG as the number of cells in the cortex cell file from the Quiescent center (QC) to the first elongated cell (Casamitjana-Martínez et al., 2003). The samples were mounted with clearing solution (80 g chloral hydrate, 30 mL glycerol, and 10 mL dH_2O) and observed immediately. The main root length was determined 11 DAG using ImageJ software (http://imagej.nih.gov/ij/). At least 23 seedlings of each line were analyzed.

Leaf Phenotype Analysis

Plants, 24 DAG in soil at 21°C under a 16-h light/8-h dark regime with a light intensity of 75 μmol m^{-2} s^{-1}were used for leaf series on 1% agar plates, picture taking, and image analysis of leaf lamina area, length, and width as described (Cnops et al., 2004). Leaf 3 was chosen for epidermal cell imaging because of its full expansion at 24 DAG (Fig. 4C; Pyke et al., 1991; Medford et al., 1992). Leaves were fixed overnight in 100% ethanol and mounted with 90% lactic acid. The leaf area was measured with the ImageJ software. The epidermal cells on the abaxial side were drawn with a Leica DMLB microscope equipped with a drawing tube and differential interference contrast objectives. The total number of cells per leaf was calculated as described previously (De Veylder et al., 2001). We estimated the total number of cells per leaf by dividing the leaf area by the mean cell area (averaged between the tip and basal positions). Means between samples were compared by a two-tailed Student's *t* test.

Enzymatic Activity Measurement (XDH)

XDH1 activity measurements in plant crude extracts were performed as described in Hesberg et al. (2004). Briefly, total protein extract was obtained from 10-d-old Arabidopsis seedlings. Plant tissue was grown in liquid nitrogen, resuspended in two volumes of extraction buffer (100 mM Tris-HCl pH 7.5, 2.5 mM EDTA, 5 mM DTT), and centrifuged. Supernatants were concentrated using Nanosep centrifugal devices (30K Omega, Pall Life Sciences) and 100 μg of total protein quantified by the method of Bradford (1976) were used for activity assays. Four to sixteen percent native polyacrylamide gels under nonreducing conditions were run at 4°C, followed by in-gel staining with 1 mM hypoxanthine, 1 mM 3-(4,5-dimethyl-2-thiazolyl)-2,5-diphenyltetrazolium bromide, and 0.1 mM phenazine methosulfate in 250 mM Tris-HCl, pH 8.5.

Metabolite Profiling by Gas Chromatography/Time of Flight-Mass Spectrometry

Metabolite analysis by gas chromatography-mass spectrometry was performed essentially as described by Lisec et al. (2006) by injecting metabolite extracts from 1 mg fresh weight of plant material into the gas chromatograph/time of flight-mass spectrometer. Chromatograms and mass spectra were evaluated using Xcalibur 2.1 software (Thermo Fisher Scientific). Specific fragment and expected elution time of target metabolites (urea, allantoic acid, allantoin, hypoxanthine, uric acid, xanthine, and xanthosine) were identified by coelution with authentic standards. Peak areas of the mass (*m/z*) fragments were normalized to the internal standard (ribitol) and fresh weight of the samples. Identification and annotation of detected peaks are shown in Supplemental Table S2 following recent recommendations for reporting metabolite data (Fernie et al., 2011).

Pathogen Infection

Cultivation and spore harvesting of *Botrytis cinerea* strain B05.10 (provided by Rudi Aerts, Katholieke Hogeschool Kempen, Belgium) was performed as described previously (Broekaert et al., 1990). Arabidopsis wild-type (Col-0) and mutants plants were grown for 4 weeks in soil ("DCM potgrond voor Zaaien en Stekken"; DCM, Sint-Katelijne-Waver, Belgium) in a growth chamber at 21°C, 75% humidity, and a 12-h day/light cycle with a light intensity of approximately 120 μmol m^{-2} s^{-1}. A 5-μL drop of a *B. cinerea* spore suspension (5×10^5/mL in half-strength potato dextrose broth) was inoculated on three leaves per plant. Plants were kept in transparent, sealed boxes to retain almost 100% humidity after inoculation. Disease symptoms were scored by measuring the diameter of the necrotic lesions at 2 and 3 d postinoculation. Thirty-two plants per line were analyzed. Two independent assays with similar results were performed.

Accession Numbers

Accession numbers of the genes used in this study are as follows: GRXS17, AT4G04950; MET18, AT5G48120; DRE2, AT5G18400; NAR1, AT4G16440; CIA1, AT2G26060; AE7/CIA2, AT1G68310; XDH1, AT4G34890; URH1, AT2G36310; URH2, AT1G05620; UREG, AT2G34470; CTU1, AT2G44270; CTU1L, AT1G76170; CTU2, AT4G35910; ELO3, AT5G50320; Leu-tRNA ligase, AT1G09620; PARP2, AT4G02390; ACC2, AT1G36180; GMI, AT5G24280; F4P13.14, AT3G01600; AAA-ATPase, AT2G18193; and DTX3, AT2G04050 and AT5G60250.

Supplemental Data

The following supplemental materials are available.

Supplemental Figure S1. GRXS17 interacts with DRE2 and XDH1 in planta.

Supplemental Figure S2. Characterization of the *grxs17* mutants used in this study.

Supplemental Figure S3. Analysis of the functioning of the purine salvage pathway in *grxs17-1* seedlings.

Supplemental Figure S4. BIFC controls.

Supplemental Figure S5. *grxs17* and *elo3-6* mutants have similar developmental defects.

Supplemental Figure S6. *grxs17* and *elo3-6* mutants show similar molecular defects.

Supplemental Table S1. RNA-Seq analysis of the *grxs17-1* mutant.

Supplemental Table S2. Identification and annotation of detected purine metabolite peaks.

Supplemental Table S3. Primers used in this study.

Supplemental Dataset S1. Mass spectrometry data of TAP experiments.

ACKNOWLEDGMENTS

We thank Florian Bittner for providing the *XDH1* clone, Frederik Coppens for support with the RNA-Seq analysis, Pia Neyt for technical support, and Annick Bleys for help in preparing the manuscript.

Received February 19, 2016; accepted August 3, 2016; published August 8, 2016.

LITERATURE CITED

Anders S, Pyl PT, Huber W (2015) HTSeq—a Python framework to work with high-throughput sequencing data. Bioinformatics **31:** 166–169

Arabidopsis Interactome Mapping Consortium (2011) Evidence for network evolution in an Arabidopsis interactome map. Science **333:** 601–607

Ascencio-Ibáñez JT, Sozzani R, Lee TJ, Chu TM, Wolfinger RD, Cella R, Hanley-Bowdoin L (2008) Global analysis of Arabidopsis gene expression uncovers a complex array of changes impacting pathogen response and cell cycle during geminivirus infection. Plant Physiol **148:** 436–454

Balk J, Schaedler TA (2014) Iron cofactor assembly in plants. Annu Rev Plant Biol **65:** 125–153

Banci L, Ciofi-Baffoni S, Gajda K, Muzzioli R, Peruzzini R, Winkelmann J (2015) N-terminal domains mediate [2Fe-2S] cluster transfer from glutaredoxin-3 to anamorsin. Nat Chem Biol **11:** 772–778

Benjamini Y, Hochberg Y (1995) Controlling the false discovery rate: a practical and powerful approach to multiple testing. J R Stat Soc Series B Stat Methodol **57:** 289–300

Bernard DG, Netz DJ, Lagny TJ, Pierik AJ, Balk J (2013) Requirements of the cytosolic iron-sulfur cluster assembly pathway in Arabidopsis. Philos Trans R Soc Lond B Biol Sci **368:** 20120259

Björk GR, Huang B, Persson OP, Byström AS (2007) A conserved modified wobble nucleoside (mcm5s2U) in lysyl-tRNA is required for viability in yeast. RNA **13:** 1245–1255

Björk GR, Jacobsson K, Nilsson K, Johansson MJ, Byström AS, Persson OP (2001) A primordial tRNA modification required for the evolution of life? EMBO J **20:** 231–239

Boruc J, Van den Daele H, Hollunder J, Rombauts S, Mylle E, Hilson P, Inzé D, De Veylder L, Russinova E (2010) Functional modules in the *Arabidopsis* core cell cycle binary protein-protein interaction network. Plant Cell **22:** 1264–1280

Bouvier D, Labessan N, Clémancey M, Latour JM, Ravanat JL, Fontecave M, Atta M (2014) TtcA a new tRNA-thioltransferase with an Fe-S cluster. Nucleic Acids Res **42:** 7960–7970

Bradford MM (1976) A rapid and sensitive method for the quantitation of microgram quantities of protein utilizing the principle of protein-dye binding. Anal Biochem **72:** 248–254

Broekaert WF, Terras FRG, Cammue BPA, Vanderleyden J (1990) An automated quantitative assay for fungal growth inhibition. FEMS Microbiol Lett **69:** 55–59

Brychkova G, Alikulov Z, Fluhr R, Sagi M (2008) A critical role for ureides in dark and senescence-induced purine remobilization is unmasked in the Atxdh1 Arabidopsis mutant. Plant J **54:** 496–509

Casamitjana-Martínez E, Hofhuis HF, Xu J, Liu CM, Heidstra R, Scheres B (2003) Root-specific CLE19 overexpression and the sol1/2 suppressors implicate a CLV-like pathway in the control of Arabidopsis root meristem maintenance. Curr Biol **13:** 1435–1441

Chen C, Huang B, Eliasson M, Rydén P, Byström AS (2011) Elongator complex influences telomeric gene silencing and DNA damage response by its role in wobble uridine tRNA modification. PLoS Genet **7:** e1002258

Cheng NH, Liu JZ, Liu X, Wu Q, Thompson SM, Lin J, Chang J, Whitham SA, Park S, Cohen JD, et al (2011) Arabidopsis monothiol glutaredoxin, AtGRXS17, is critical for temperature-dependent postembryonic growth and development via modulating auxin response. J Biol Chem **286:** 20398–20406

Circelli P, Donini M, Villani ME, Benvenuto E, Marusic C (2010) Efficient *Agrobacterium*-based transient expression system for the production of biopharmaceuticals in plants. Bioeng Bugs **1:** 221–224

Clough SJ, Bent AF (1998) Floral dip: a simplified method for Agrobacterium-mediated transformation of Arabidopsis thaliana. Plant J **16:** 735–743

Cnops G, Jover-Gil S, Peters JL, Neyt P, De Block S, Robles P, Ponce MR, Gerats T, Micol JL, Van Lijsebettens M (2004) The rotunda2 mutants identify a role for the LEUNIG gene in vegetative leaf morphogenesis. J Exp Bot **55:** 1529–1539

Couturier J, Przybyla-Toscano J, Roret T, Didierjean C, Rouhier N (2015) The roles of glutaredoxins ligating Fe-S clusters: Sensing, transfer or repair functions? Biochim Biophys Acta **1853:** 1513–1527

Couturier J, Touraine B, Briat JF, Gaymard F, Rouhier N (2013) The iron-sulfur cluster assembly machineries in plants: current knowledge and open questions. Front Plant Sci **4:** 259

Couturier J, Wu HC, Dhalleine T, Pégeot H, Sudre D, Gualberto JM, Jacquot JP, Gaymard F, Vignols F, Rouhier N (2014) Monothiol glutaredoxin-BolA interactions: redox control of Arabidopsis thaliana BolA2 and SufE1. Mol Plant **7:** 187–205

Cuéllar Pérez A, Pauwels L, De Clercq R, Goossens A (2013) Yeast two-hybrid analysis of jasmonate signaling proteins. Methods Mol Bio. **1011:** 173–186

De Veylder L, Beeckman T, Beemster GT, Krols L, Terras F, Landrieu I, van der Schueren E, Maes S, Naudts M, Inzé D (2001) Functional analysis of cyclin-dependent kinase inhibitors of Arabidopsis. Plant Cell **13:** 1653–1668

DeFraia CT, Wang Y, Yao J, Mou Z (2013) Elongator subunit 3 positively regulates plant immunity through its histone acetyltransferase and radical S-adenosylmethionine domains. BMC Plant Biol **13:** 102

DeFraia CT, Zhang X, Mou Z (2010) Elongator subunit 2 is an accelerator of immune responses in Arabidopsis thaliana. Plant J **64:** 511–523

Duan CG, Wang X, Tang K, Zhang H, Mangrauthia SK, Lei M, Hsu CC, Hou YJ, Wang C, Li Y, et al (2015) MET18 connects the cytosolic iron-sulfur cluster assembly pathway to active DNA demethylation in arabidopsis. PLoS Genet **11:** e1005559

Fernie AR, Aharoni A, Willmitzer L, Stitt M, Tohge T, Kopka J, Carroll AJ, Saito K, Fraser PD, DeLuca V (2011) Recommendations for reporting metabolite data. Plant Cell **23:** 2477–2482

Gari K, León Ortiz AM, Borel V, Flynn H, Skehel JM, Boulton SJ (2012) MMS19 links cytoplasmic iron-sulfur cluster assembly to DNA metabolism. Science **337:** 243–245

Gerber J, Neumann K, Prohl C, Mühlenhoff U, Lill R (2004) The yeast scaffold proteins Isu1p and Isu2p are required inside mitochondria for maturation of cytosolic Fe/S proteins. Mol Cell Biol **24:** 4848–4857

Goodman HM, Olson MV, Hall BD (1977) Nucleotide sequence of a mutant eukaryotic gene: the yeast tyrosine-inserting ochre suppressor SUP4-o. Proc Natl Acad Sci USA **74:** 5453–5457

Han YF, Huang HW, Li L, Cai T, Chen S, He XJ (2015) The cytosolic iron-sulfur cluster assembly protein MMS19 regulates transcriptional gene silencing, DNA repair, and flowering time in Arabidopsis. PLoS One **10:** e0129137

Haunhorst P, Berndt C, Eitner S, Godoy JR, Lillig CH (2010) Characterization of the human monothiol glutaredoxin 3 (PICOT) as iron-sulfur protein. Biochem Biophys Res Commun **394:** 372–376

Haunhorst P, Hanschmann EM, Bräutigam L, Stehling O, Hoffmann B, Mühlenhoff U, Lill R, Berndt C, Lillig CH (2013) Crucial function of vertebrate glutaredoxin 3 (PICOT) in iron homeostasis and hemoglobin maturation. Mol Biol Cell **24:** 1895–1903

Herrero E, de la Torre-Ruiz MA (2007) Monothiol glutaredoxins: a common domain for multiple functions. Cell Mol Life Sci **64:** 1518–1530

Hesberg C, Hänsch R, Mendel RR, Bittner F (2004) Tandem orientation of duplicated xanthine dehydrogenase genes from Arabidopsis thaliana: differential gene expression and enzyme activities. J Biol Chem **279:** 13547–13554

Huang B, Johansson MJ, Byström AS (2005) An early step in wobble uridine tRNA modification requires the Elongator complex. RNA **11:** 424–436

Igloi GL (1988) Interaction of tRNAs and of phosphorothioate-substituted nucleic acids with an organomercurial. Probing the chemical environment of thiolated residues by affinity electrophoresis. Biochemistry **27:** 3842–3849

Isakov N, Witte S, Altman A (2000) PICOT-HD: a highly conserved protein domain that is often associated with thioredoxin and glutaredoxin modules. Trends Biochem Sci **25:** 537–539

Jablonowski D, Frohloff F, Fichtner L, Stark MJ, Schaffrath R (2001) Kluyveromyces lactis zymocin mode of action is linked to RNA polymerase II function via Elongator. Mol Microbiol **42:** 1095–1105

Jablonowski D, Schaffrath R (2007) Zymocin, a composite chitinase and tRNase killer toxin from yeast. Biochem Soc Trans **35:** 1533–1537

Jablonowski D, Täubert JE, Bär C, Stark MJ, Schaffrath R (2009) Distinct subsets of Sit4 holophosphatases are required for inhibition of Saccharomyces cerevisiae growth by rapamycin and zymocin. Eukaryot Cell **8:** 1637–1647

Jablonowski D, Zink S, Mehlgarten C, Daum G, Schaffrath R (2006) tRNAGlu wobble uridine methylation by Trm9 identifies Elongator's key role for zymocin-induced cell death in yeast. Mol Microbiol **59:** 677–688

Jäger G, Leipuviene R, Pollard MG, Qian Q, Björk GR (2004) The conserved Cys-X1-X2-Cys motif present in the TtcA protein is required for the thiolation of cytidine in position 32 of tRNA from Salmonella enterica serovar Typhimurium. J Bacteriol **186:** 750–757

Kalhor HR, Clarke S (2003) Novel methyltransferase for modified uridine residues at the wobble position of tRNA. Mol Cell Biol **23:** 9283–9292

Karimi M, De Meyer B, Hilson P (2005) Modular cloning in plant cells. Trends Plant Sci **10:** 103–105

Kispal G, Csere P, Prohl C, Lill R (1999) The mitochondrial proteins Atm1p and Nfs1p are essential for biogenesis of cytosolic Fe/S proteins. EMBO J **18:** 3981–3989

Knuesting J, Riondet C, Maria C, Kruse I, Bécuwe N, König N, Berndt C, Tourrette S, Guilleminot-Montoya J, Herrero E, et al (2015) Arabidopsis glutaredoxin S17 and its partner, the nuclear factor Y subunit C11/negative cofactor 2α, contribute to maintenance of the shoot apical meristem under long-day photoperiod. Plant Physiol **167:** 1643–1658

Leiber RM, John F, Verhertbruggen Y, Diet A, Knox JP, Ringli C (2010) The TOR pathway modulates the structure of cell walls in Arabidopsis. Plant Cell **22:** 1898–1908

Leidel S, Pedrioli PG, Bucher T, Brost R, Costanzo M, Schmidt A, Aebersold R, Boone C, Hofmann K, Peter M (2009) Ubiquitin-related modifier Urm1 acts as a sulphur carrier in thiolation of eukaryotic transfer RNA. Nature **458:** 228–232

Leihne V, Kirpekar F, Vågbø CB, van den Born E, Krokan HE, Grini PE, Meza TJ, Falnes PO (2011) Roles of Trm9- and ALKBH8-like proteins in the formation of modified wobble uridines in Arabidopsis tRNA. Nucleic Acids Res **39:** 7688–7701

Leitner J, Retzer K, Malenica N, Bartkeviciute R, Lucyshyn D, Jäger G, Korbei B, Byström A, Luschnig C (2015) Meta-regulation of Arabidopsis auxin responses depends on tRNA maturation. Cell Reports **11:** 516–526

Li H, Mapolelo DT, Dingra NN, Naik SG, Lees NS, Hoffman BM, Riggs-Gelasco PJ, Huynh BH, Johnson MK, Outten CE (2009) The yeast iron regulatory proteins Grx3/4 and Fra2 form heterodimeric complexes containing a [2Fe-2S] cluster with cysteinyl and histidyl ligation. Biochemistry **48:** 9569–9581

Li H, Mapolelo DT, Randeniya S, Johnson MK, Outten CE (2012) Human glutaredoxin 3 forms [2Fe-2S]-bridged complexes with human BolA2. Biochemistry **51:** 1687–1696

Lisec J, Schauer N, Kopka J, Willmitzer L, Fernie AR (2006) Gas chromatography mass spectrometry-based metabolite profiling in plants. Nat Protoc **1:** 387–396

Lu J, Huang B, Esberg A, Johansson MJ, Byström AS (2005) The Kluyveromyces lactis gamma-toxin targets tRNA anticodons. RNA **11:** 1648–1654

Luo D, Bernard DG, Balk J, Hai H, Cui X (2012) The DUF59 family gene AE7 acts in the cytosolic iron-sulfur cluster assembly pathway to maintain nuclear genome integrity in Arabidopsis. Plant Cell **24:** 4135–4148

Medford JI, Behringer FJ, Callos JD, Feldmann KA (1992) Normal and abnormal development in the Arabidopsis vegetative shoot apex. Plant Cell **4:** 631–643

Mehlgarten C, Jablonowski D, Wrackmeyer U, Tschitschmann S, Sondermann D, Jäger G, Gong Z, Byström AS, Schaffrath R, Breunig KD (2010) Elongator function in tRNA wobble uridine modification is conserved between yeast and plants. Mol Microbiol **76:** 1082–1094

Mortimer RK, Johnston JR (1986) Genealogy of principal strains of the yeast genetic stock center. Genetics **113:** 35–43

Mühlenhoff U, Molik S, Godoy JR, Uzarska MA, Richter N, Seubert A, Zhang Y, Stubbe J, Pierrel F, Herrero E, et al (2010) Cytosolic monothiol glutaredoxins function in intracellular iron sensing and trafficking via their bound iron-sulfur cluster. Cell Metab **12:** 373–385

Nakagawa A, Sakamoto S, Takahashi M, Morikawa H, Sakamoto A (2007) The RNAi-mediated silencing of xanthine dehydrogenase impairs growth and fertility and accelerates leaf senescence in transgenic Arabidopsis plants. Plant Cell Physiol **48:** 1484–1495

Nakai Y, Nakai M, Lill R, Suzuki T, Hayashi H (2007) Thio modification of yeast cytosolic tRNA is an iron-sulfur protein-dependent pathway. Mol Cell Biol **27:** 2841–2847

Nandakumar J, Schwer B, Schaffrath R, Shuman S (2008) RNA repair: an antidote to cytotoxic eukaryal RNA damage. Mol Cell **31:** 278–286

Nedialkova DD, Leidel SA (2015) Optimization of codon translation rates via tRNA modifications maintains proteome integrity. Cell **161:** 1606–1618

Nelissen H, De Groeve S, Fleury D, Neyt P, Bruno L, Bitonti MB, Vandenbussche F, Van der Straeten D, Yamaguchi T, Tsukaya H, et al (2010) Plant Elongator regulates auxin-related genes during RNA polymerase II transcription elongation. Proc Natl Acad Sci USA **107:** 1678–1683

Nelissen H, Fleury D, Bruno L, Robles P, De Veylder L, Traas J, Micol JL, Van Montagu M, Inzé D, Van Lijsebettens M (2005) The elongata mutants identify a functional Elongator complex in plants with a role in cell proliferation during organ growth. Proc Natl Acad Sci USA **102:** 7754–7759

Paraskevopoulou C, Fairhurst SA, Lowe DJ, Brick P, Onesti S (2006) The Elongator subunit Elp3 contains a Fe4S4 cluster and binds S-adenosylmethionine. Mol Microbiol **59:** 795–806

Philipp M, John F, Ringli C (2014) The cytosolic thiouridylase CTU2 of Arabidopsis thaliana is essential for posttranscriptional thiolation of tRNAs and influences root development. BMC Plant Biol **14:** 109

Picciocchi A, Saguez C, Boussac A, Cassier-Chauvat C, Chauvat F (2007) CGFS-type monothiol glutaredoxins from the cyanobacterium Synechocystis PCC6803 and other evolutionary distant model organisms possess a glutathione-ligated [2Fe-2S] cluster. Biochemistry **46:** 15018–15026

Pujol-Carrion N, Belli G, Herrero E, Nogues A, de la Torre-Ruiz MA (2006) Glutaredoxins Grx3 and Grx4 regulate nuclear localisation of Aft1 and the oxidative stress response in Saccharomyces cerevisiae. J Cell Sci **119:** 4554–4564

Pyke KA, Marrison JL, Leech RM (1991) Temporal and spatial development of the cells of the expanding first leaf of Arabidopsis thaliana (L.) Heynh. J Exp Bot **42:** 1407–1416

Riegler H, Geserick C, Zrenner R (2011) Arabidopsis thaliana nucleosidase mutants provide new insights into nucleoside degradation. New Phytol **191:** 349–359

Robinson MD, McCarthy DJ, Smyth GK (2010) edgeR: a Bioconductor package for differential expression analysis of digital gene expression data. Bioinformatics **26:** 139–140

Robinson MD, Smyth GK (2008) Small-sample estimation of negative binomial dispersion, with applications to SAGE data. Biostatistics **9:** 321–332

Rolland T, Taşan M, Charloteaux B, Pevzner SJ, Zhong Q, Sahni N, Yi S, Lemmens I, Fontanillo C, Mosca R, et al (2014) A proteome-scale map of the human interactome network. Cell **159:** 1212–1226

Roret T, Tsan P, Couturier J, Zhang B, Johnson MK, Rouhier N, Didierjean C (2014) Structural and spectroscopic insights into BolA-glutaredoxin complexes. J Biol Chem **289:** 24588–24598

Rual JF, Venkatesan K, Hao T, Hirozane-Kishikawa T, Dricot A, Li N, Berriz GF, Gibbons FD, Dreze M, Ayivi-Guedehoussou N, et al (2005) Towards a proteome-scale map of the human protein-protein interaction network. Nature **437:** 1173–1178

Saito Y, Shibayama H, Tanaka H, Tanimura A, Matsumura I, Kanakura Y (2011) PICOT is a molecule which binds to anamorsin. Biochem Biophys Res Commun **408:** 329–333

Scheidt V, Jüdes A, Bar CB, Klassen R, Schaffrath R (2014) Loss of wobble uridine modification in tRNA anticodons interferes with TOR pathway signaling. Microb Cell **1:** 416–424

Schlieker CD, Van der Veen AG, Damon JR, Spooner E, Ploegh HL (2008) A functional proteomics approach links the ubiquitin-related modifier Urm1 to a tRNA modification pathway. Proc Natl Acad Sci USA **105:** 18255–18260

Selvadurai K, Wang P, Seimetz J, Huang RH (2014) Archaeal Elp3 catalyzes tRNA wobble uridine modification at C5 via a radical mechanism. Nat Chem Biol **10:** 810–812

Shaw KJ, Olson MV (1984) Effects of altered 5′-flanking sequences on the in vivo expression of a Saccharomyces cerevisiae tRNATyr gene. Mol Cell Biol **4:** 657–665

Sheftel A, Stehling O, Lill R (2010) Iron-sulfur proteins in health and disease. Trends Endocrinol Metab **21:** 302–314

Sherman F (2002) Getting started with yeast. Methods Enzymol **350:** 3–41

Stehling O, Mascarenhas J, Vashisht AA, Sheftel AD, Niggemeyer B, Rösser R, Pierik AJ, Wohlschlegel JA, Lill R (2013) Human CIA2A-FAM96A

and CIA2B-FAM96B integrate iron homeostasis and maturation of different subsets of cytosolic-nuclear iron-sulfur proteins. Cell Metab **18:** 187–198

Stehling O, Vashisht AA, Mascarenhas J, Jonsson ZO, Sharma T, Netz DJ, Pierik AJ, Wohlschlegel JA, Lill R (2012) MMS19 assembles iron-sulfur proteins required for DNA metabolism and genomic integrity. Science **337:** 195–199

Tarassov K, Messier V, Landry CR, Radinovic S, Serna Molina MM, Shames I, Malitskaya Y, Vogel J, Bussey H, Michnick SW (2008) An in vivo map of the yeast protein interactome. Science **320:** 1465–1470

Van Leene J, Eeckhout D, Cannoot B, De Winne N, Persiau G, Van De Slijke E, Vercruysse L, Dedecker M, Verkest A, Vandepoele K, et al (2015) An improved toolbox to unravel the plant cellular machinery by tandem affinity purification of Arabidopsis protein complexes. Nat Protoc **10:** 169–187

Van Leene J, Eeckhout D, Persiau G, Van De Slijke E, Geerinck J, Van Isterdael G, Witters E, De Jaeger G (2011) Isolation of transcription factor complexes from Arabidopsis cell suspension cultures by tandem affinity purification. Methods Mol Biol **754:** 195–218

van Wietmarschen N, Moradian A, Morin GB, Lansdorp PM, Uringa EJ (2012) The mammalian proteins MMS19, MIP18, and ANT2 are involved in cytoplasmic iron-sulfur cluster protein assembly. J Biol Chem **287:** 43351–43358

Wang C, Ding Y, Yao J, Zhang Y, Sun Y, Colee J, Mou Z (2015) Arabidopsis Elongator subunit 2 positively contributes to resistance to the necrotrophic fungal pathogens Botrytis cinerea and Alternaria brassicicola. Plant J **83:** 1019–1033

Watanabe S, Nakagawa A, Izumi S, Shimada H, Sakamoto A (2010) RNA interference-mediated suppression of xanthine dehydrogenase reveals the role of purine metabolism in drought tolerance in Arabidopsis. FEBS Lett **584:** 1181–1186

Witte CP, Rosso MG, Romeis T (2005) Identification of three urease accessory proteins that are required for urease activation in Arabidopsis. Plant Physiol **139:** 1155–1162

Wu Q, Lin J, Liu JZ, Wang X, Lim W, Oh M, Park J, Rajashekar CB, Whitham SA, Cheng NH, et al (2012) Ectopic expression of Arabidopsis glutaredoxin AtGRXS17 enhances thermotolerance in tomato. Plant Biotechnol J **10:** 945–955

Wu TD, Nacu S (2010) Fast and SNP-tolerant detection of complex variants and splicing in short reads. Bioinformatics **26:** 873–881

Xia H, Li B, Zhang Z, Wang Q, Qiao T, Li K (2015) Human glutaredoxin 3 can bind and effectively transfer [4Fe-4S] cluster to apo-iron regulatory protein 1. Biochem Biophys Res Commun **465:** 620–624

Xu D, Huang W, Li Y, Wang H, Huang H, Cui X (2012) Elongator complex is critical for cell cycle progression and leaf patterning in Arabidopsis. Plant J **69:** 792–808

Zarepour M, Kaspari K, Stagge S, Rethmeier R, Mendel RR, Bittner F (2010) Xanthine dehydrogenase AtXDH1 from Arabidopsis thaliana is a potent producer of superoxide anions via its NADH oxidase activity. Plant Mol Biol **72:** 301–310

Zhang Y, Liu L, Wu X, An X, Stubbe J, Huang M (2011) Investigation of in vivo diferric tyrosyl radical formation in Saccharomyces cerevisiae Rnr2 protein: requirement of Rnr4 and contribution of Grx3/4 AND Dre2 proteins. J Biol Chem **286:** 41499–41509

Zinshteyn B, Gilbert WV (2013) Loss of a conserved tRNA anticodon modification perturbs cellular signaling. PLoS Genet **9:** e1003675

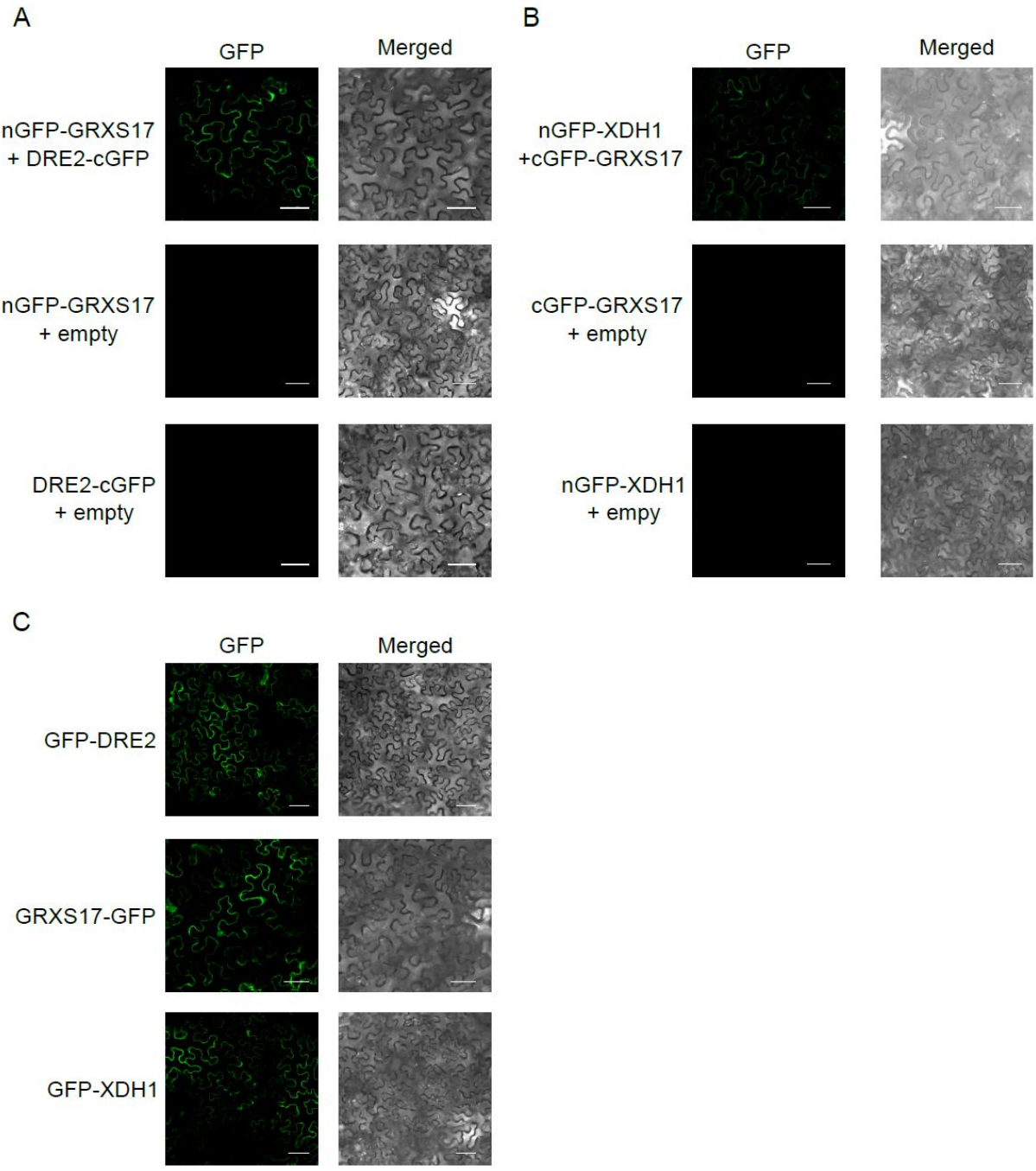

Figure S1. GRXS17 interacts with DRE2 and XDH1 *in planta*. A and B, GRXS17 interaction with DRE2 (A) and XDH1 (B) by bimolecular fluorescence complementation. Fusion proteins with an N-terminal (nGFP) or C-terminal (cGFP) fragment of GFP were transiently co-expressed in *N. benthamiana* leaves and analyzed by confocal microscopy, three days after agro-infiltration. C, Confocal microscopy images of *N. benthamiana* leaves transiently expressing *GFP-DRE2* or *GRXS17-GFP* and *GFP-XDH1*. Scale bars: 50 μm.

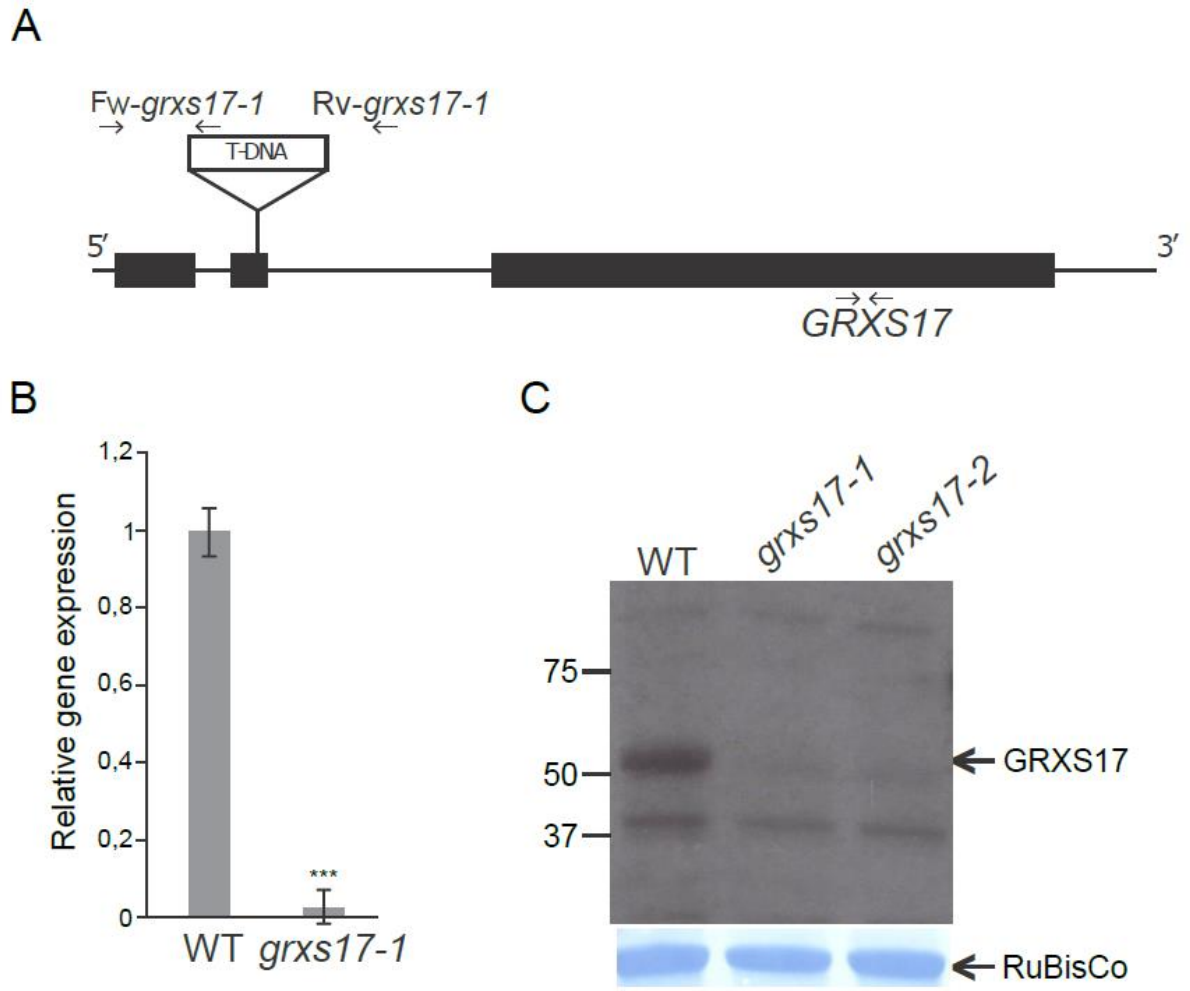

Figure S2. Characterization of the *grxs17* mutants used in this study. A, Schematic visualization of the *GRXS17* gene structure. Black boxes represent exons. T-DNA insertion and primers used for genotyping and qRT-PCR are indicated above or below, respectively. B, *GRXS17* gene expression analysis by qRT-PCR in *grxs17-1* seedlings. The *GRXS17* expression ratio relative to that in wild-type Col-0 seedlings is plotted (set at 1). Bars represent means ±SE of n=3 (***, $P<0.001$, Student's t-test). C, Immunoblot analysis with a polyclonal anti-GRXS17 antiserum showing the absence of GRXS17 proteins in *grxs17-1* and *grxs17-2* seedlings.

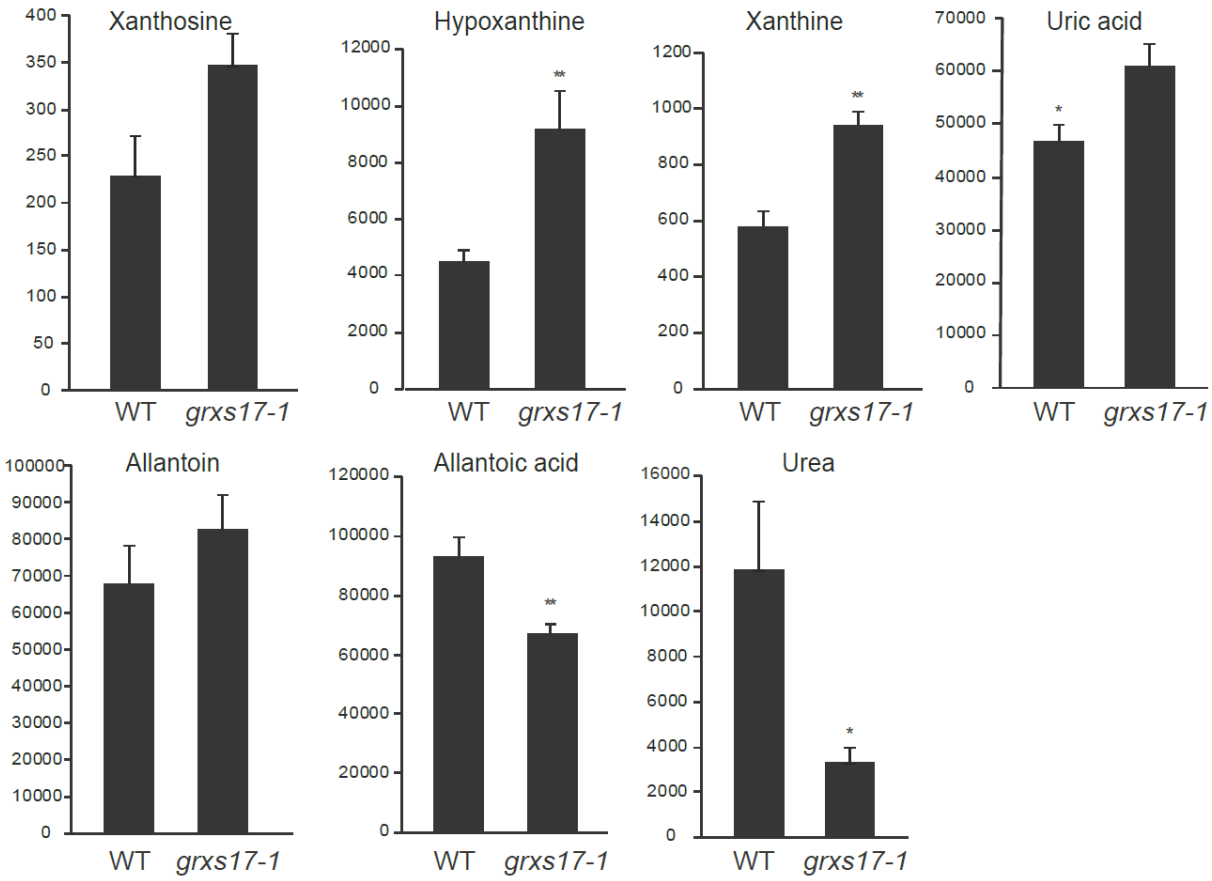

Figure S3. Analysis of the functioning of the purine salvage pathway in *grxs17-1* seedlings. Quantification of purine degradation intermediates in 10-day-old seedlings grown on MS media supplemented with 1% sucrose. The y-axes correspond to the relative peak areas representing specific mass fragment ion peaks (described in Supplemental Table S2) that were normalized by fresh weight and peak area of the internal standard. Bars represent means ±SE of n=5 (*, P<0.05; **, P<0.01; Student's t-test).

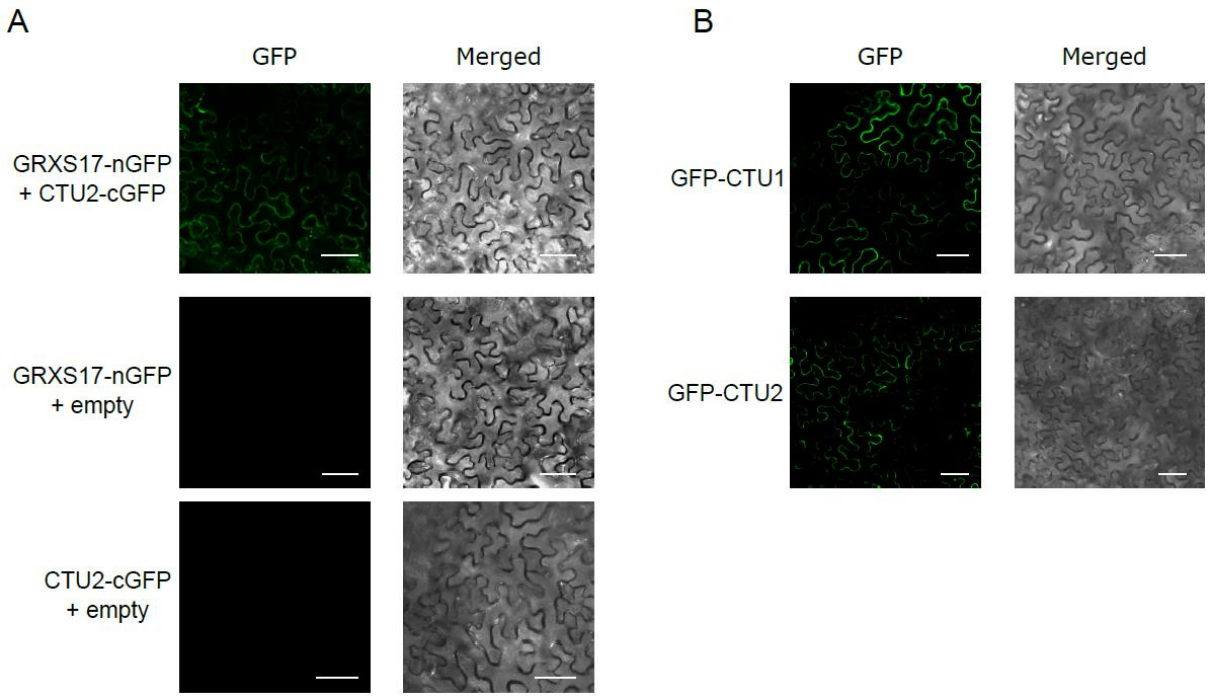

Figure S4. BIFC controls. A, Controls for CTU2 interaction with GRXS17 by bimolecular fluorescence complementation. Fusion proteins with an N-terminal (nGFP) or C-terminal (cGFP) fragment of GFP were transiently expressed in *N. benthamiana* leaves and analyzed by confocal microscopy, three days after agro-infiltration. B, Confocal microscopy images of *N. benthamiana* leaves transiently expressing *GFP-CTU2* or *GFP-CTU2.* Scale bars: 50 μm.

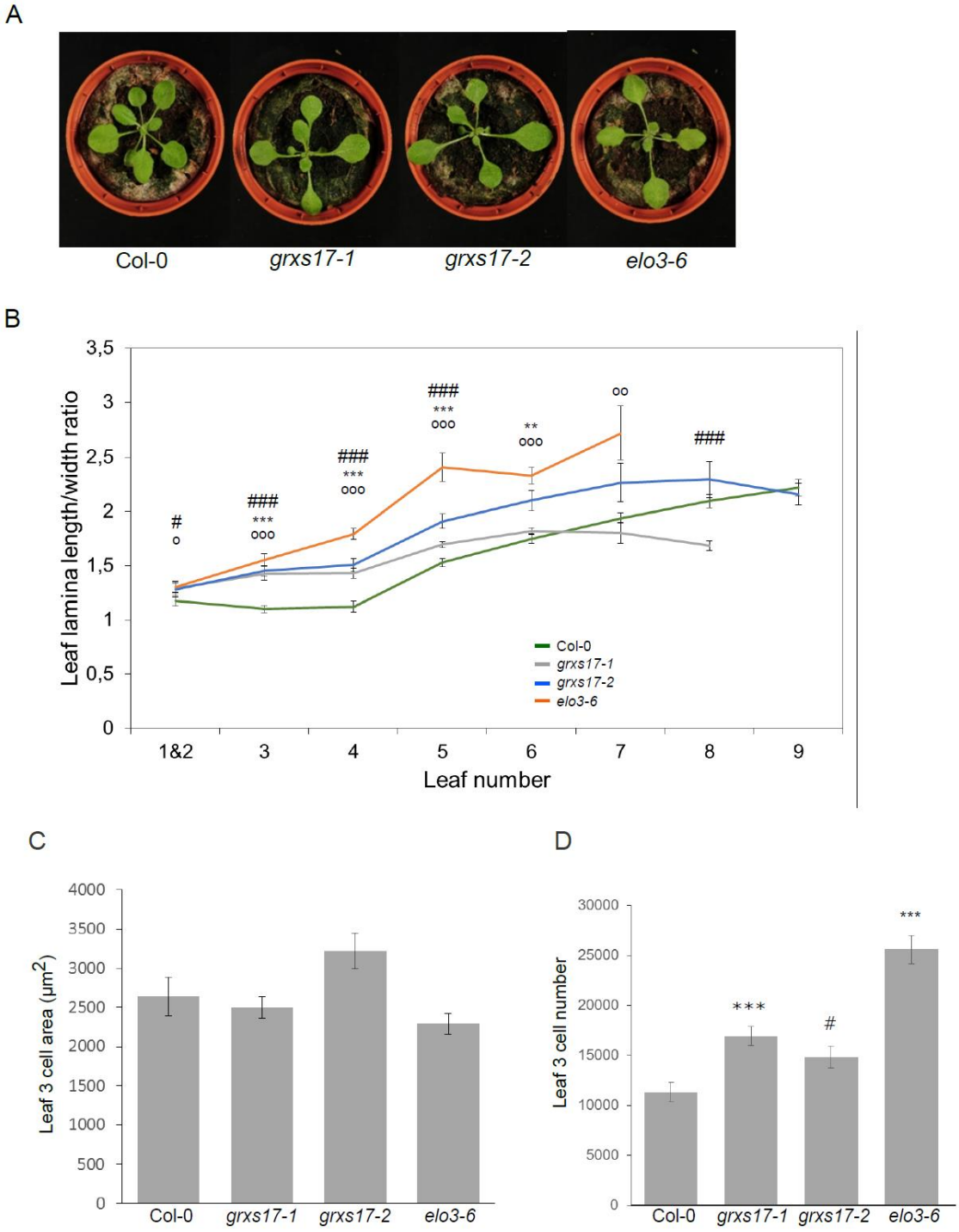

Figure S5. *grxs17* and *elo3-6* mutants have similar developmental defects. A, Representative plant phenotypes, 19 days after germination (DAG) of left to right: Col-0, *grxs17-1*, grxs17-2 and *elo3-6*. B, Ratio between leaf lamina length and width of leaf series of plants, 24 DAG, grown in soil (n≥10) (*, P<0.05; **, P<0.01; ***, P<0.001, Student's t-test, # comparison between Col-0 and *grxs17-1*; * for Col-0 and *grxs17-2* and ^{o} for Col-0 and *elo3-6*. C and D, Cellular analysis of leaf 3 (n=5): mean of cell area (C) and calculated number of cells (D) (***, P<0.001; #, P=0.06, Student's t-test). Bars represent SE.

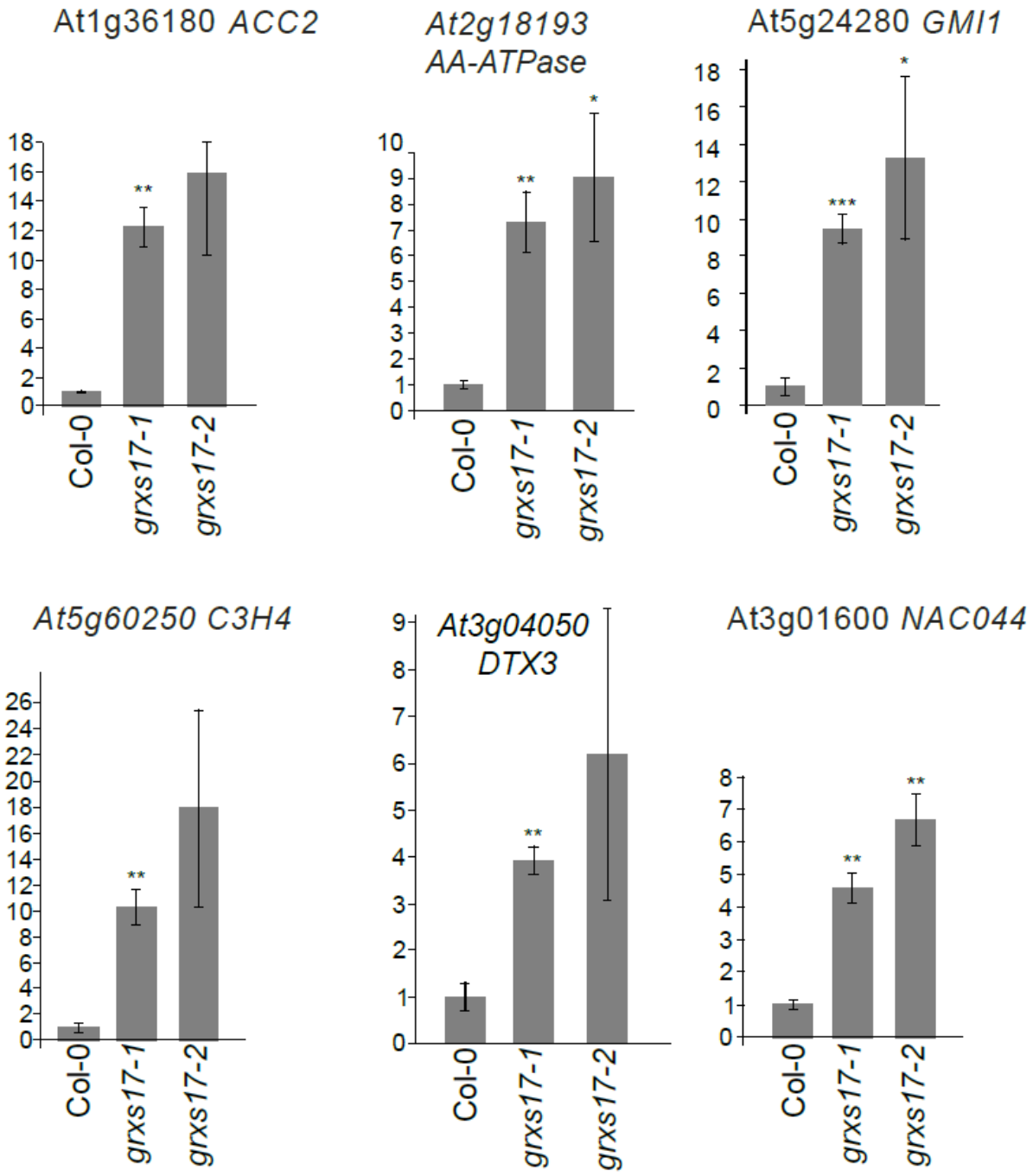

Figure S6. *grxs17* and *elo3-6* mutants show similar molecular defects. qPCR validation of gene expression in *grxs17-1* and *grxs17-2*. The expression ratio relative to that in wild-type Col-0 seedlings is plotted (set at 1). Bars represent means ±SE of n=3 (*, P<0.05; **, P<0.01; ***, P<0.001, Student's t-test).

Table S1. Differentially expressed genes obtained by RNA-Sequencing analysis of the *grxs17-1* loss-of-function seedlings.

Locus	logFC	logCPM	PValue	FDR	Short description
AT2G03130	7,8431	-0,9583	1,64E-23	4,36E-21	Ribosomal protein L12/ ATP-dependent Clp protease adaptor protein ClpS family protein
AT2G24255	7,5244	-1,2068	1,41E-19	2,61E-17	Protein of unknown function (DUF295)
AT1G30170	6,7259	0,9718	2,32E-73	5,05E-70	Protein of unknown function (DUF295)
AT4G17710	5,9496	-0,9566	2,33E-23	5,94E-21	homeodomain GLABROUS 4 (HDG4)
AT5G53230	5,1691	1,1845	5,76E-80	1,41E-76	Protein of unknown function (DUF295)
AT5G14490	4,9533	-0,6570	2,03E-24	5,85E-22	NAC domain containing protein 85 (NAC085)
AT5G55270	4,7198	-0,0076	2,91E-33	1,78E-30	Protein of unknown function (DUF295)
AT5G59390	4,6879	-0,2682	3,65E-30	1,66E-27	XH/XS domain-containing protein
AT5G54560	4,6639	-1,3435	1,14E-15	1,52E-13	Protein of unknown function (DUF295)
AT5G53240	4,6525	-0,9294	2,67E-19	4,80E-17	Protein of unknown function (DUF295)
AT3G01345	4,4126	0,2226	1,98E-40	1,62E-37	Expressed protein
AT4G05380	4,3607	0,0290	1,26E-33	8,00E-31	P-loop containing nucleoside triphosphate hydrolases superfamily protein
AT5G60250	4,3006	2,8474	1,98E-145	1,29E-141	zinc finger (C3HC4-type RING finger) family protein
AT4G05370	4,2930	-0,6389	1,14E-21	2,66E-19	BCS1 AAA-type ATPase
AT2G20800	4,1930	2,0061	2,66E-91	8,69E-88	NAD(P)H dehydrogenase B4 (NDB4)
AT4G22470	3,9753	2,9779	4,65E-13	4,16E-11	protease inhibitor/seed storage/lipid transfer protein (LTP) family protein
AT3G01600	3,7631	3,0316	7,30E-144	3,58E-140	NAC domain containing protein 44 (NAC044)
AT2G18720	3,6950	-0,4126	1,82E-23	4,76E-21	Translation elongation factor EF1A/initiation factor IF2gamma family protein
AT2G39030	3,6676	0,4972	4,77E-08	1,93E-06	Acyl-CoA N-acyltransferases (NAT) superfamily protein
AT4G12490	3,6453	3,2611	3,06E-20	6,18E-18	Bifunctional inhibitor/lipid-transfer protein/seed storage 2S albumin superfamily protein
AT3G22860	3,0983	-0,7617	4,34E-14	4,45E-12	eukaryotic translation initiation factor 3 subunit C2 (TIF3C2)
AT5G47000	3,0965	-0,0307	1,80E-21	4,11E-19	Peroxidase superfamily protein
AT4G32510	3,0591	-1,4097	3,57E-10	2,11E-08	HCO3- transporter family
AT5G20240	3,0528	-0,8197	1,06E-14	1,19E-12	PISTILLATA (PI)
AT4G12480	2,9736	6,9036	1,06E-57	1,57E-54	pEARLI 1
AT5G58610	2,9158	1,6751	9,47E-58	1,55E-54	PHD finger transcription factor, putative
AT5G13210	2,8400	3,3197	2,04E-87	5,73E-84	Uncharacterised conserved protein UCP015417, vWA
AT3G54530	2,8270	-0,3893	4,72E-16	6,61E-14	unknown protein
AT4G12470	2,8266	4,8391	1,06E-28	4,17E-26	azelaic acid induced 1 (AZI1)

32	AT5G24280	2,8123	4,1506	1,02E-127	4,00E-124	GAMMA-IRRADIATION AND MITOMYCIN C INDUCED 1 (GMI1)
33	AT3G18610	2,7156	1,9487	1,12E-57	1,57E-54	nucleolin like 2 (NUC-L2)
34	AT5G64060	2,6805	1,8069	7,69E-54	9,42E-51	NAC domain containing protein 103 (NAC103)
35	AT1G36180	2,6310	5,8323	6,22E-167	6,10E-163	acetyl-CoA carboxylase 2 (ACC2)
36	AT1G03710	2,5470	-0,9329	1,63E-10	1,02E-08	Cystatin/monellin superfamily protein
37	AT4G21680	2,4794	1,2493	6,10E-20	1,17E-17	NITRATE TRANSPORTER 1.8 (NRT1.8)
38	AT1G17960	2,4753	2,4977	1,75E-66	3,43E-63	Threonyl-tRNA synthetase
39	AT1G11070	2,4537	2,2998	5,34E-51	5,81E-48	Similar to Hydroxyproline-rich glycoprotein family protein
40	AT1G30160	2,4404	0,8004	6,13E-29	2,50E-26	Protein of unknown function (DUF295)
41	AT1G49570	2,4232	3,1231	6,18E-57	8,07E-54	Peroxidase superfamily protein
42	AT5G24640	2,3760	0,4693	3,29E-21	7,19E-19	unknown protein
43	AT5G09570	2,3161	1,7229	1,58E-39	1,24E-36	Cox19-like CHCH family protein
44	AT1G05490	2,2963	0,7971	1,71E-25	5,25E-23	chromatin remodeling 31 (chr31)
45	AT2G18190	2,2698	-0,5504	1,49E-11	1,10E-09	P-loop containing nucleoside triphosphate hydrolases superfamily protein
46	AT5G44575	2,2674	0,1789	2,43E-11	1,72E-09	unknown protein
47	AT5G07200	2,1916	0,0057	1,44E-15	1,88E-13	gibberellin 20-oxidase 3 (GA20OX3)
48	AT5G12030	2,1478	-0,4739	4,01E-11	2,72E-09	heat shock protein 17.6A (HSP17.6A)
49	AT3G58270	2,1348	2,4710	4,66E-51	5,37E-48	Arabidopsis phospholipase-like protein (PEARLI 4) with TRAF-like domain
50	AT2G47520	2,1346	-0,1203	8,29E-15	9,52E-13	HYPOXIA RESPONSIVE ERF (ETHYLENE RESPONSE FACTOR) 2 (HRE2)
51	AT5G58840	2,1010	-0,7230	2,76E-09	1,42E-07	Subtilase family protein
52	AT2G18193	2,0929	4,6821	3,26E-38	2,46E-35	P-loop containing nucleoside triphosphate hydrolases superfamily protein
53	AT1G20350	2,0614	-0,6479	3,49E-10	2,08E-08	translocase inner membrane subunit 17-1 (TIM17-1)
54	AT1G76470	2,0370	-0,6079	1,02E-09	5,65E-08	NAD(P)-binding Rossmann-fold superfamily protein
55	AT1G70260	2,0312	2,0482	5,53E-33	3,29E-30	nodulin MtN21 /EamA-like transporter family protein
56	AT1G30660	2,0098	-0,9147	8,56E-08	3,25E-06	unknown protein
57	AT3G27620	1,9986	-0,0357	1,32E-12	1,13E-10	alternative oxidase 1C (AOX1C)
58	AT2G38340	1,9289	0,0990	8,10E-14	8,10E-12	Integrase-type DNA-binding superfamily protein
59	AT4G12735	1,9024	-0,2646	1,12E-09	6,14E-08	unknown protein
60	AT3G09950	1,8924	-0,4923	1,03E-09	5,70E-08	unknown protein
61	AT5G51440	1,8907	2,9705	4,93E-46	5,09E-43	HSP20-like chaperones superfamily protein
62	AT2G21450	1,8832	-0,6898	1,61E-08	7,23E-07	chromatin remodeling 34 (CHR34)

63	AT1G18100	1,8678	2,3204	1,17E-24	3,48E-22	E12A11
64	AT2G21640	1,8663	2,4958	2,10E-30	9,79E-28	unknown protein
65	AT4G15350	1,8526	-0,7776	8,00E-08	3,06E-06	cytochrome P450, family 705, subfamily A, polypeptide 2 (CYP705A2)
66	AT2G41730	1,8312	2,7400	1,39E-36	9,41E-34	unknown protein
67	AT1G65570	1,8228	0,6566	1,68E-17	2,72E-15	Pectin lyase-like superfamily protein
68	AT1G53540	1,7874	-0,5366	6,84E-08	2,66E-06	HSP20-like chaperones superfamily protein
69	AT4G16590	1,7828	-0,6030	4,41E-08	1,80E-06	cellulose synthase-like A01 (CSLA01)
70	AT1G70440	1,7752	0,8400	4,33E-18	7,20E-16	similar to RCD one 3 (SRO3)
71	AT1G20400	1,7694	0,7318	6,06E-15	7,11E-13	FUNCTIONS IN: molecular_function unknown
72	AT2G38250	1,7461	1,0757	2,73E-20	5,57E-18	Homeodomain-like superfamily protein
73	AT3G46230	1,7274	0,7771	2,46E-13	2,31E-11	heat shock protein 17.4 (HSP17.4)
74	AT5G19470	1,7022	2,7655	5,44E-09	2,65E-07	nudix hydrolase homolog 24 (NUDT24)
75	AT3G28580	1,6985	1,3791	1,19E-11	8,96E-10	P-loop containing nucleoside triphosphate hydrolases superfamily protein
76	AT1G49920	1,6932	-0,8888	1,97E-06	5,28E-05	MuDR family transposase
77	AT1G61255	1,6724	-0,8046	6,06E-07	1,86E-05	Similar to glycine-rich protein
78	AT1G67760	1,6513	0,6887	4,77E-15	5,84E-13	TCP-1/cpn60 chaperonin family protein
79	AT5G11410	1,6440	0,7932	1,66E-14	1,81E-12	Protein kinase superfamily protein
80	AT2G04050	1,6328	3,8197	1,93E-14	2,06E-12	MATE efflux family protein
81	AT1G65500	1,6113	1,4600	3,21E-13	2,97E-11	unknown protein
82	AT5G67060	1,6049	-0,2688	1,73E-08	7,72E-07	HECATE 1 (HEC1)
83	AT5G25230	1,5970	0,9286	4,52E-16	6,38E-14	Ribosomal protein S5/Elongation factor G/III/V family protein
84	AT1G52120	1,5967	3,2178	1,04E-28	4,17E-26	Mannose-binding lectin superfamily protein
85	AT4G36570	1,5946	0,9778	2,13E-12	1,75E-10	RAD-like 3 (RL3)
86	AT2G42430	1,5888	1,0904	3,22E-17	4,96E-15	lateral organ boundaries-domain 16 (LBD16)
87	AT1G18835	1,5868	-0,8893	5,81E-06	1,35E-04	MINI ZINC FINGER 3 (MIF3)
88	AT4G30250	1,5855	0,7416	2,27E-05	4,44E-04	P-loop containing nucleoside triphosphate hydrolases superfamily protein
89	AT1G53130	1,5774	0,6593	3,27E-13	3,01E-11	GRIM REAPER (GRI)
90	AT3G45730	1,5712	2,2311	2,70E-24	7,67E-22	unknown protein
91	AT3G47030	1,5694	-0,0415	4,69E-09	2,31E-07	F-box and associated interaction domains-containing protein
92	AT1G54890	1,5664	0,8721	3,84E-14	3,98E-12	Late embryogenesis abundant (LEA) protein-related
93	AT5G19700	1,5645	1,4530	1,95E-18	3,30E-16	MATE efflux family protein

94	AT4G20690	1,5636	-0,3952	7,10E-08	2,75E-06	unknown protein
95	AT4G15210	1,5388	2,4580	1,74E-15	2,23E-13	beta-amylase 5 (BAM5)
96	AT2G44570	1,5291	0,8942	7,31E-15	8,49E-13	glycosyl hydrolase 9B12 (GH9B12)
97	AT3G21720	1,4924	2,1238	4,06E-13	3,67E-11	isocitrate lyase (ICL)
98	AT5G67430	1,4863	2,8286	5,21E-20	1,02E-17	Acyl-CoA N-acyltransferases (NAT) superfamily protein
99	AT1G66920	1,4782	0,6856	1,04E-10	6,75E-09	Protein kinase superfamily protein
100	AT5G37490	1,4712	-0,8576	5,53E-05	9,57E-04	ARM repeat superfamily protein
101	AT3G59930	1,4592	-0,7282	1,06E-05	2,28E-04	FUNCTIONS IN: molecular_function unknown
102	AT1G19380	1,4538	1,0789	3,89E-08	1,60E-06	Protein of unknown function (DUF1195)
103	AT2G23170	1,4324	3,1675	1,62E-31	8,61E-29	GH3.3
104	AT5G44574	1,4300	-0,6117	7,97E-06	1,78E-04	unknown protein
105	AT5G46050	1,4238	0,0951	1,71E-06	4,66E-05	peptide transporter 3 (PTR3)
106	AT1G52060	1,4216	3,9461	9,97E-38	7,24E-35	Mannose-binding lectin superfamily protein
107	AT4G33970	1,4064	-0,6773	1,76E-05	3,58E-04	Leucine-rich repeat (LRR) family protein
108	AT1G64160	1,4019	0,1512	3,73E-08	1,54E-06	Disease resistance-responsive (dirigent-like protein) family protein
109	AT4G02700	1,3892	1,3765	5,50E-15	6,57E-13	SULFATE TRANSPORTER 3;2
110	AT4G15160	1,3807	6,5393	2,11E-15	2,69E-13	Bifunctional inhibitor/lipid-transfer protein/seed storage 2S albumin superfamily protein
111	AT3G11260	1,3767	-0,7107	2,10E-05	4,15E-04	WUSCHEL related homeobox 5 (WOX5)
112	AT3G48520	1,3548	1,7855	5,27E-16	7,28E-14	cytochrome P450, family 94, subfamily B, polypeptide 3 (CYP94B3)
113	AT4G22960	1,3530	0,4665	1,31E-08	5,97E-07	Protein of unknown function (DUF544)
114	AT4G11720	1,3369	-0,7358	4,02E-05	7,33E-04	HAPLESS 2 (HAP2)
115	AT3G14060	1,3310	2,7325	6,70E-16	9,12E-14	unknown protein
116	AT3G20710	1,3242	-0,3587	3,46E-05	6,43E-04	F-box family protein
117	AT1G52070	1,3060	4,9117	2,99E-26	9,93E-24	Mannose-binding lectin superfamily protein
118	AT1G61800	1,3046	1,7120	4,32E-16	6,13E-14	glucose-6-phosphate/phosphate translocator 2 (GPT2)
119	AT2G32830	1,3018	-0,8245	6,91E-05	1,16E-03	Encodes Pht1
120	AT3G08860	1,2867	4,8593	1,75E-42	1,49E-39	PYRIMIDINE 4 (PYD4)
121	AT2G04070	1,2790	0,2872	1,21E-07	4,42E-06	MATE efflux family protein
122	AT3G22142	1,2738	6,1850	1,37E-21	3,16E-19	Bifunctional inhibitor/lipid-transfer protein/seed storage 2S albumin superfamily protein
123	AT3G24780	1,2735	1,2546	8,11E-13	7,10E-11	Uncharacterised conserved protein UCP015417, vWA
124	AT5G55110	1,2731	0,4314	7,67E-07	2,29E-05	Stigma-specific Stig1 family protein

125	AT1G76930	1,2718	8,2336	2,02E-24	5,85E-22	extensin 4 (EXT4)
126	AT2G34340	1,2705	0,8270	1,31E-10	8,38E-09	Protein of unknown function, DUF584
127	AT1G52040	1,2676	5,2807	4,34E-21	9,35E-19	myrosinase-binding protein 1 (MBP1)
128	AT3G13130	1,2666	-0,7931	1,42E-04	2,11E-03	unknown protein
129	AT3G04320	1,2614	1,4747	4,93E-14	5,01E-12	Kunitz family trypsin and protease inhibitor protein
130	AT3G52780	1,2561	-0,6598	4,49E-05	8,04E-04	PAP20
131	AT4G38340	1,2488	0,0141	1,41E-06	3,96E-05	Plant regulator RWP-RK family protein
132	AT4G30140	1,2473	5,6542	1,19E-25	3,75E-23	CUTICLE DESTRUCTING FACTOR 1 (CDEF1)
133	AT2G38823	1,2451	1,0749	2,01E-09	1,06E-07	unknown protein
134	AT3G45060	1,2406	-0,4820	1,77E-05	3,60E-04	high affinity nitrate transporter 2.6 (NRT2.6)
135	AT3G13080	1,2397	6,2305	9,98E-44	9,31E-41	multidrug resistance-associated protein 3 (MRP3)
136	AT4G06746	1,2280	-0,0902	3,52E-06	8,77E-05	related to AP2 9 (RAP2.9)
137	AT3G58190	1,2241	-0,9177	8,01E-04	8,61E-03	lateral organ boundaries-domain 29 (LBD29)
138	AT3G21520	1,2209	0,5942	6,23E-09	3,00E-07	DUF679 domain membrane protein 1 (DMP1)
139	AT1G68480	1,2169	-0,2766	4,98E-06	1,19E-04	JAGGED (JAG)
140	AT3G14700	1,2141	-0,5033	6,55E-05	1,11E-03	SART-1 family
141	AT5G61740	1,2083	0,3148	1,01E-07	3,72E-06	ABC2 homolog 14 (ATH14)
142	AT4G01985	1,2070	1,7042	1,27E-05	2,68E-04	unknown protein
143	AT5G58390	1,1941	3,0264	7,78E-09	3,66E-07	Peroxidase superfamily protein
144	AT3G48700	1,1923	1,5956	1,43E-12	1,22E-10	carboxyesterase 13 (CXE13)
145	AT1G34460	1,1906	-0,9363	6,62E-04	7,46E-03	B1 type cyclin
146	AT1G27020	1,1844	2,0929	1,49E-04	2,20E-03	unknown protein
147	AT5G48850	1,1749	3,6637	5,39E-19	9,44E-17	SULPHUR DEFICIENCY-INDUCED 1 (ATSDI1)
148	AT2G27550	1,1703	2,9705	3,96E-18	6,63E-16	centroradialis (ATC)
149	AT5G12330	1,1676	3,2921	2,95E-11	2,05E-09	LATERAL ROOT PRIMORDIUM 1 (LRP1)
150	AT5G38700	1,1664	-0,1246	2,05E-05	4,06E-04	unknown protein
151	AT3G19200	1,1633	0,1635	7,24E-07	2,18E-05	unknown protein
152	AT1G24260	1,1613	0,0822	1,76E-06	4,78E-05	SEPALLATA3 (SEP3)
153	AT5G44568	1,1566	-0,1104	1,25E-05	2,64E-04	unknown protein
154	AT2G43590	1,1538	6,2958	1,68E-13	1,61E-11	Chitinase family protein
155	AT4G13680	1,1516	-0,0465	9,14E-06	2,00E-04	Protein of unknown function (DUF295)

156	AT5G63090	1,1422	0,7759	2,46E-07	8,38E-06	LATERAL ORGAN BOUNDARIES (LOB)
157	AT5G60520	1,1360	2,5943	9,96E-16	1,33E-13	Late embryogenesis abundant (LEA) protein-related
158	AT1G13330	1,1330	1,0768	1,18E-09	6,45E-08	Arabidopsis Hop2 homolog (AHP2)
159	AT1G03660	1,1276	-0,4460	6,79E-05	1,14E-03	Ankyrin-repeat containing protein
160	AT3G62270	1,1246	5,8965	2,87E-11	2,01E-09	HCO3- transporter family
161	AT1G52770	1,1192	0,4271	4,09E-07	1,31E-05	Phototropic-responsive NPH3 family protein
162	AT1G24095	1,1189	2,1256	6,03E-15	7,11E-13	Putative thiol-disulphide oxidoreductase DCC
163	AT1G43910	1,1135	2,4765	3,53E-15	4,38E-13	P-loop containing nucleoside triphosphate hydrolases superfamily protein
164	AT1G19630	1,0978	0,4228	5,04E-07	1,58E-05	cytochrome P450, family 722, subfamily A, polypeptide 1 (CYP722A1)
165	AT4G16240	1,0960	-0,2926	1,02E-04	1,62E-03	unknown protein
166	AT3G49580	1,0863	4,2018	1,16E-13	1,14E-11	RESPONSE TO LOW SULFUR 1 (LSU1)
167	AT4G16563	1,0837	3,0586	3,32E-14	3,46E-12	Eukaryotic aspartyl protease family protein
168	AT1G69310	1,0802	3,6718	2,17E-22	5,25E-20	WRKY DNA-binding protein 57 (WRKY57)
169	AT5G20820	1,0797	0,2187	2,89E-06	7,37E-05	SAUR-like auxin-responsive protein family
170	AT3G27630	1,0785	-0,8287	1,23E-03	1,20E-02	unknown protein
171	AT3G15720	1,0762	1,5566	2,73E-11	1,92E-09	Pectin lyase-like superfamily protein
172	AT4G14780	1,0761	0,2935	7,71E-06	1,73E-04	Protein kinase superfamily protein
173	AT4G16600	1,0748	0,2866	3,06E-06	7,75E-05	Nucleotide-diphospho-sugar transferases superfamily protein
174	AT4G23130	1,0697	-0,4296	5,99E-04	6,88E-03	cysteine-rich RLK (RECEPTOR-like protein kinase) 5 (CRK5)
175	AT2G18600	1,0673	1,6474	2,32E-11	1,64E-09	Ubiquitin-conjugating enzyme family protein
176	AT5G13330	1,0615	2,6651	4,88E-16	6,79E-14	related to AP2 6l (Rap2.6L)
177	AT3G62460	1,0506	3,4776	2,44E-12	1,99E-10	Putative endonuclease or glycosyl hydrolase
178	AT3G13210	1,0443	-0,3164	1,62E-04	2,37E-03	crooked neck protein, putative / cell cycle protein, putative
179	AT3G61630	1,0412	3,6366	2,21E-20	4,61E-18	cytokinin response factor 6 (CRF6)
180	AT5G39580	1,0361	2,8709	1,74E-13	1,65E-11	Peroxidase superfamily protein
181	AT5G18180	1,0347	-0,6141	5,93E-04	6,82E-03	H/ACA ribonucleoprotein complex, subunit Gar1/Naf1 protein
182	AT3G28500	1,0311	-0,4333	2,18E-04	3,03E-03	60S acidic ribosomal protein family
183	AT3G05660	1,0295	0,9974	5,07E-08	2,04E-06	receptor like protein 33 (RLP33)
184	AT5G60040	1,0288	4,3056	4,74E-27	1,66E-24	nuclear RNA polymerase C1 (NRPC1)
185	AT3G44300	1,0195	6,4975	2,95E-26	9,93E-24	nitrilase 2 (NIT2)
186	AT5G19880	1,0158	0,1457	7,14E-05	1,19E-03	Peroxidase superfamily protein

187	AT4G22710	1,0111	0,7508	7,39E-07	2,22E-05	cytochrome P450, family 706, subfamily A, polypeptide 2 (CYP706A2)
188	AT1G20620	1,0100	10,4325	4,03E-24	1,11E-21	catalase 3 (CAT3)
189	AT2G36270	1,0057	0,3976	4,88E-06	1,17E-04	ABA INSENSITIVE 5 (ABI5)
190	AT5G52940	1,0028	0,8410	3,51E-07	1,15E-05	Protein of unknown function (DUF295)
191	AT4G20235	-1,0020	-0,8017	1,91E-03	1,69E-02	cytochrome P450, family 71, subfamily A, polypeptide 28 (CYP71A28)
192	AT5G53380	-1,0025	-0,8501	2,19E-03	1,89E-02	O-acyltransferase (WSD1-like) family protein
193	AT4G04700	-1,0048	1,3951	6,54E-09	3,13E-07	calcium-dependent protein kinase 27 (CPK27)
194	AT1G24130	-1,0048	-0,0500	2,61E-04	3,54E-03	Transducin/WD40 repeat-like superfamily protein
195	AT1G12570	-1,0092	2,2742	7,33E-11	4,85E-09	Glucose-methanol-choline (GMC) oxidoreductase family protein
196	AT1G14220	-1,0100	0,3891	4,83E-06	1,16E-04	Ribonuclease T2 family protein
197	AT5G38710	-1,0203	1,8201	1,42E-11	1,06E-09	Methylenetetrahydrofolate reductase family protein
198	AT3G29630	-1,0206	1,5082	1,25E-09	6,78E-08	UDP-Glycosyltransferase superfamily protein
199	AT4G12520	-1,0207	2,5350	2,07E-12	1,71E-10	Bifunctional inhibitor/lipid-transfer protein/seed storage 2S albumin superfamily protein
200	AT3G12460	-1,0216	-0,6949	1,64E-03	1,51E-02	Polynucleotidyl transferase, ribonuclease H-like superfamily protein
201	AT3G13610	-1,0229	5,8197	2,13E-23	5,49E-21	2-oxoglutarate (2OG) and Fe(II)-dependent oxygenase superfamily protein
202	AT5G67090	-1,0235	0,3223	5,45E-06	1,28E-04	Subtilisin-like serine endopeptidase family protein
203	AT3G45430	-1,0283	1,3272	9,13E-10	5,13E-08	Concanavalin A-like lectin protein kinase family protein
204	AT5G59360	-1,0294	0,7129	3,15E-07	1,03E-05	unknown protein
205	AT5G65030	-1,0298	-0,0636	1,20E-04	1,84E-03	unknown protein
206	AT5G45960	-1,0312	1,1336	1,12E-08	5,14E-07	GDSL-like Lipase/Acylhydrolase superfamily protein
207	AT3G05155	-1,0320	0,0818	1,38E-05	2,89E-04	Major facilitator superfamily protein
208	AT5G10946	-1,0328	0,7462	4,04E-07	1,30E-05	unknown protein
209	AT5G53250	-1,0341	3,3419	2,62E-13	2,44E-11	arabinogalactan protein 22 (AGP22)
210	AT5G18050	-1,0344	0,9515	1,41E-07	5,08E-06	SAUR-like auxin-responsive protein family
211	AT3G09960	-1,0387	0,3340	3,35E-06	8,38E-05	Calcineurin-like metallo-phosphoesterase superfamily protein
212	AT5G62340	-1,0392	2,5366	7,04E-12	5,47E-10	Plant invertase/pectin methylesterase inhibitor superfamily protein
213	AT5G39110	-1,0473	-0,8864	1,68E-03	1,54E-02	RmlC-like cupins superfamily protein
214	AT2G43440	-1,0510	-0,1713	3,59E-05	6,63E-04	F-box and associated interaction domains-containing protein
215	AT5G40990	-1,0515	-0,5197	3,79E-04	4,76E-03	GDSL lipase 1 (GLIP1)
216	AT2G18800	-1,0536	1,7143	8,47E-12	6,49E-10	xyloglucan endotransglucosylase/hydrolase 21 (XTH21)
217	AT4G04760	-1,0573	-0,7666	1,62E-03	1,50E-02	Major facilitator superfamily protein

218	AT3G09400	-1,0574	0,1178	2,78E-05	5,29E-04	pol-like 3 (PLL3)
219	AT5G46900	-1,0582	4,0158	7,05E-25	2,13E-22	Bifunctional inhibitor/lipid-transfer protein/seed storage 2S albumin superfamily protein
220	AT5G42510	-1,0587	1,2436	7,50E-08	2,89E-06	Disease resistance-responsive (dirigent-like protein) family protein
221	AT2G41480	-1,0594	2,4384	9,87E-15	1,11E-12	Peroxidase superfamily protein
222	AT1G18970	-1,0594	3,4860	2,47E-22	5,90E-20	germin-like protein 4 (GLP4)
223	AT2G24310	-1,0649	-0,5752	8,13E-04	8,72E-03	unknown protein
224	AT3G55900	-1,0673	-0,6467	5,24E-04	6,19E-03	F-box family protein
225	AT1G16530	-1,0693	1,6295	3,67E-11	2,52E-09	ASYMMETRIC LEAVES 2-like 9 (ASL9)
226	AT3G47220	-1,0705	0,9287	1,45E-08	6,59E-07	phosphatidylinositol-speciwc phospholipase C9 (PLC9)
227	AT5G63140	-1,0714	2,3215	5,80E-14	5,86E-12	purple acid phosphatase 29 (PAP29)
228	AT2G38995	-1,0746	2,4936	1,88E-14	2,03E-12	O-acyltransferase (WSD1-like) family protein
229	AT2G04800	-1,0777	1,4511	4,48E-10	2,64E-08	unknown protein
230	ATCG00810	-1,0798	-0,6254	3,88E-04	4,85E-03	ribosomal protein L22 (RPL22)
231	AT3G52770	-1,0801	-0,1099	5,67E-05	9,76E-04	LITTLE ZIPPER 3 (ZPR3)
232	AT2G40960	-1,0811	3,1766	2,81E-21	6,32E-19	Single-stranded nucleic acid binding R3H protein
233	AT1G63520	-1,0821	0,2984	8,90E-06	1,96E-04	Protein of unknown function (DUF3527)
234	AT1G17147	-1,0842	1,5033	1,37E-11	1,02E-09	VQ motif-containing protein
235	AT5G49780	-1,0851	0,9635	7,15E-09	3,39E-07	Leucine-rich repeat protein kinase family protein
236	AT3G29430	-1,0854	-0,4161	1,31E-04	1,98E-03	Terpenoid synthases superfamily protein
237	AT2G18470	-1,0917	1,3664	2,85E-10	1,74E-08	roline-rich extensin-like receptor kinase 4 (PERK4)
238	AT5G43230	-1,0967	0,2060	3,16E-06	7,94E-05	unknown protein
239	AT5G42600	-1,1031	4,0057	1,20E-25	3,75E-23	marneral synthase (MRN1)
240	AT2G18690	-1,1115	2,5207	3,30E-11	2,28E-09	unknown protein
241	AT1G52890	-1,1122	-0,1563	5,44E-05	9,45E-04	NAC domain containing protein 19 (NAC019)
242	AT1G28480	-1,1153	-0,0084	1,06E-05	2,28E-04	GRX480
243	AT5G57010	-1,1195	1,2466	1,58E-10	9,93E-09	calmodulin-binding family protein
244	AT5G65690	-1,1237	1,1879	7,40E-10	4,20E-08	phosphoenolpyruvate carboxykinase 2 (PCK2)
245	AT1G66090	-1,1266	0,0648	2,24E-05	4,38E-04	Disease resistance protein (TIR-NBS class)
246	AT2G30432	-1,1268	0,0545	5,20E-06	1,23E-04	TRICHOMELESS1 (TCL1)
247	AT3G48940	-1,1283	-1,0066	2,29E-03	1,95E-02	Remorin family protein
248	AT3G19615	-1,1319	-0,7102	1,54E-04	2,27E-03	unknown protein

249	AT1G10340	-1,1382	0,1564	4,20E-06	1,03E-04	Ankyrin repeat family protein
250	AT5G56970	-1,1425	-1,0816	3,63E-03	2,76E-02	cytokinin oxidase 3 (CKX3)
251	AT1G66270	-1,1439	6,4364	1,49E-37	1,04E-34	BGLU21
252	AT1G26380	-1,1446	2,2712	2,99E-14	3,16E-12	FAD-binding Berberine family protein
253	AT3G22910	-1,1472	-0,0154	5,63E-06	1,31E-04	ATPase E1-E2 type family protein / haloacid dehalogenase-like hydrolase family protein
254	AT4G36880	-1,1490	2,0825	7,32E-15	8,49E-13	cysteine proteinase1 (CP1)
255	AT1G13550	-1,1502	-1,1018	1,95E-03	1,72E-02	Protein of unknown function (DUF1262)
256	AT4G23493	-1,1506	0,4891	1,65E-07	5,79E-06	unknown protein
257	AT5G49770	-1,1506	0,1634	1,87E-06	5,03E-05	Leucine-rich repeat protein kinase family protein
258	AT2G01520	-1,1556	7,6398	3,15E-21	7,01E-19	owering.
259	AT5G51470	-1,1582	-0,5327	1,68E-04	2,44E-03	Auxin-responsive GH3 family protein
260	AT2G38600	-1,1589	-0,0932	4,35E-06	1,06E-04	HAD superfamily, subfamily IIIB acid phosphatase
261	AT3G01260	-1,1596	3,5702	2,53E-28	9,74E-26	Galactose mutarotase-like superfamily protein
262	ATCG00800	-1,1698	0,0952	1,64E-06	4,50E-05	RESISTANCE TO PSEUDOMONAS SYRINGAE 3 (RPS3)
263	AT1G62280	-1,1709	1,8365	6,13E-12	4,81E-10	SLAC1 homologue 1 (SLAH1)
264	AT5G38970	-1,1790	0,1946	1,60E-06	4,42E-05	brassinosteroid-6-oxidase 1 (BR6OX1)
265	AT1G15050	-1,1829	-0,8399	5,01E-04	5,96E-03	indole-3-acetic acid inducible 34 (IAA34)
266	AT5G23030	-1,1839	-0,3150	9,72E-06	2,11E-04	tetraspanin12 (TET12)
267	AT1G63295	-1,1839	1,2409	1,44E-10	9,16E-09	Remorin family protein
268	AT4G24340	-1,1846	1,9909	1,19E-14	1,32E-12	Phosphorylase superfamily protein
269	AT1G21550	-1,1850	0,0975	2,76E-06	7,06E-05	Calcium-binding EF-hand family protein
270	AT5G47450	-1,1934	3,6940	8,37E-12	6,43E-10	TONOPLAST INTRINSIC PROTEIN 2;3 (TIP2;3)
271	AT1G29270	-1,1950	-0,2486	2,03E-05	4,02E-04	unknown protein
272	AT3G45860	-1,1950	0,7122	6,80E-09	3,24E-07	cysteine-rich RLK (RECEPTOR-like protein kinase) 4 (CRK4)
273	AT4G15480	-1,1951	0,5771	2,52E-08	1,08E-06	UGT84A1
274	AT5G59680	-1,2039	1,7169	1,47E-14	1,61E-12	Leucine-rich repeat protein kinase family protein
275	AT4G01895	-1,2077	-0,6976	1,77E-04	2,54E-03	systemic acquired resistance (SAR) regulator protein NIMIN-1-related
276	AT3G55890	-1,2153	0,7965	3,44E-09	1,74E-07	Yippee family putative zinc-binding protein
277	AT5G13320	-1,2206	2,2826	1,53E-16	2,24E-14	AVRPPHB SUSCEPTIBLE 3 (PBS3)
278	AT5G25250	-1,2219	1,7383	5,69E-15	6,76E-13	SPFH/Band 7/PHB domain-containing membrane-associated protein family
279	AT1G66020	-1,2270	0,4517	2,04E-08	8,94E-07	Terpenoid cyclases/Protein prenyltransferases superfamily protein

280	AT4G37060	-1,2279	-1,0030	4,70E-04	5,66E-03	PATATIN-like protein 5 (PLP5)
281	AT1G19510	-1,2371	-1,0787	1,69E-03	1,55E-02	RAD-like 5 (RL5)
282	AT4G40020	-1,2437	-0,0582	1,63E-06	4,49E-05	Myosin heavy chain-related protein
283	AT4G26320	-1,2468	2,8844	1,31E-09	7,09E-08	arabinogalactan protein 13 (AGP13)
284	AT1G05650	-1,2481	1,2816	5,89E-11	3,94E-09	Pectin lyase-like superfamily protein
285	AT2G24850	-1,2561	-0,3611	4,37E-06	1,06E-04	tyrosine aminotransferase 3 (TAT3)
286	AT1G65680	-1,2579	-1,0713	1,70E-03	1,56E-02	expansin B2 (EXPB2)
287	AT1G53625	-1,2616	1,9558	3,32E-13	3,04E-11	unknown protein
288	AT2G31083	-1,2649	-0,2696	4,02E-06	9,85E-05	CLAVATA3/ESR-RELATED 5 (CLE5)
289	AT5G02540	-1,2678	2,3772	4,36E-20	8,64E-18	NAD(P)-binding Rossmann-fold superfamily protein
290	AT1G73330	-1,2697	8,5723	1,56E-27	5,56E-25	drought-repressed 4 (DR4)
291	AT4G21380	-1,2715	1,8533	3,47E-15	4,36E-13	receptor kinase 3 (RK3)
292	AT5G39120	-1,2834	-0,2125	1,51E-06	4,23E-05	RmlC-like cupins superfamily protein
293	AT5G14470	-1,2859	-0,8977	2,59E-04	3,52E-03	GHMP kinase family protein
294	AT4G12545	-1,2905	3,2621	3,12E-26	1,02E-23	Bifunctional inhibitor/lipid-transfer protein/seed storage 2S albumin superfamily protein
295	AT1G52800	-1,2947	1,0146	1,83E-11	1,33E-09	2-oxoglutarate (2OG) and Fe(II)-dependent oxygenase superfamily protein
296	AT5G23990	-1,2987	3,5405	8,78E-31	4,41E-28	ferric reduction oxidase 5 (FRO5)
297	AT1G67980	-1,2987	-0,2667	1,88E-05	3,80E-04	caffeoyl-CoA 3-O-methyltransferase (CCOAMT)
298	AT5G65600	-1,2997	-0,2630	1,40E-06	3,95E-05	Concanavalin A-like lectin protein kinase family protein
299	AT4G22212	-1,3105	2,2161	1,21E-18	2,08E-16	Arabidopsis defensin-like protein
300	AT5G23830	-1,3109	4,0591	1,28E-27	4,75E-25	MD-2-related lipid recognition domain-containing protein
301	AT2G15220	-1,3116	4,1452	2,29E-29	9,96E-27	Plant basic secretory protein (BSP) family protein
302	AT1G63450	-1,3137	0,4091	4,06E-09	2,02E-07	root hair specific 8 (RHS8)
303	AT5G65340	-1,3171	-0,7314	6,60E-05	1,12E-03	Protein of unknown function, DUF617
304	AT5G35480	-1,3264	0,4694	6,73E-10	3,84E-08	unknown protein
305	AT4G25510	-1,3361	-0,9906	7,72E-05	1,28E-03	unknown protein
306	ATCG01020	-1,3397	-0,6836	6,41E-06	1,47E-04	ribosomal protein L32 (RPL32)
307	AT1G01380	-1,3410	0,0404	4,77E-08	1,93E-06	ENHANCER OF TRY AND CPC 1 (ETC1)
308	AT2G19500	-1,3413	0,3691	1,16E-08	5,30E-07	cytokinin oxidase 2 (CKX2)
309	AT4G12550	-1,3504	4,0289	3,15E-29	1,32E-26	Auxin-Induced in Root cultures 1 (AIR1)
310	AT3G21800	-1,3519	-0,7510	6,08E-05	1,04E-03	UDP-glucosyl transferase 71B8 (UGT71B8)

311	AT4G07960	-1,3583	0,7383	2,13E-11	1,53E-09	Cellulose-synthase-like C12 (CSLC12)
312	AT5G09730	-1,3663	0,4021	5,80E-09	2,80E-07	beta-xylosidase 3 (BXL3)
313	AT3G47480	-1,3676	0,6708	7,87E-11	5,19E-09	Calcium-binding EF-hand family protein
314	AT2G16230	-1,3677	-0,3527	4,97E-06	1,19E-04	O-Glycosyl hydrolases family 17 protein
315	AT5G35940	-1,3693	0,2423	3,80E-08	1,56E-06	Mannose-binding lectin superfamily protein
316	AT3G19320	-1,3708	0,1317	1,67E-08	7,48E-07	Leucine-rich repeat (LRR) family protein
317	AT1G13510	-1,3778	1,0620	1,76E-13	1,67E-11	Protein of unknown function (DUF1262)
318	AT2G46495	-1,3789	1,4571	7,31E-16	9,81E-14	RING/U-box superfamily protein
319	AT5G46890	-1,3834	3,9260	5,00E-30	2,23E-27	Bifunctional inhibitor/lipid-transfer protein/seed storage 2S albumin superfamily protein
320	AT2G28210	-1,3864	0,3070	1,23E-09	6,71E-08	alpha carbonic anhydrase 2 (ACA2)
321	AT5G02170	-1,3902	1,4776	6,93E-17	1,05E-14	Transmembrane amino acid transporter family protein
322	AT2G02300	-1,3947	-0,9436	1,21E-04	1,86E-03	phloem protein 2-B5 (PP2-B5)
323	AT3G55910	-1,3987	-0,5078	5,61E-06	1,31E-04	unknown protein
324	AT1G77520	-1,4010	3,6112	1,36E-27	4,94E-25	O-methyltransferase family protein
325	AT5G39000	-1,4076	-0,7000	1,38E-05	2,88E-04	Malectin/receptor-like protein kinase family protein
326	AT5G39670	-1,4121	1,2667	1,45E-15	1,88E-13	Calcium-binding EF-hand family protein
327	AT1G27140	-1,4190	2,4551	6,80E-24	1,85E-21	glutathione S-transferase tau 14 (GSTU14)
328	AT3G27940	-1,4210	-0,8901	4,57E-05	8,16E-04	LOB domain-containing protein 26 (LBD26)
329	AT1G18990	-1,4400	-0,6674	7,09E-06	1,62E-04	Protein of unknown function, DUF593
330	AT3G02850	-1,4428	1,4973	2,53E-17	4,00E-15	SKOR, a member of Shaker family potassium ion (K+) channel
331	AT5G53200	-1,4535	0,5258	8,40E-10	4,73E-08	TRIPTYCHON (TRY)
332	AT1G36622	-1,4614	0,6185	2,05E-11	1,48E-09	unknown protein
333	AT3G62760	-1,4667	1,1924	4,58E-13	4,12E-11	GSTF13
334	AT1G09240	-1,4684	0,1296	4,40E-09	2,17E-07	nicotianamine synthase 3 (NAS3)
335	AT3G13784	-1,4757	2,5095	3,79E-26	1,22E-23	cell wall invertase 5 (CWINV5)
336	AT5G23780	-1,4811	-0,7783	4,47E-05	8,01E-04	DOMAIN OF UNKNOWN FUNCTION 724 9 (DUF9)
337	AT4G10310	-1,4845	2,5781	2,00E-19	3,67E-17	high-affinity K+ transporter 1 (HKT1)
338	AT1G13520	-1,4874	2,4387	2,26E-20	4,67E-18	Protein of unknown function (DUF1262)
339	AT2G24720	-1,4973	0,5066	9,47E-11	6,19E-09	glutamate receptor 2.2 (GLR2.2)
340	AT1G74080	-1,5010	-0,6139	3,15E-06	7,94E-05	myb domain protein 122 (MYB122)
341	AT3G12240	-1,5059	-0,5085	2,38E-06	6,24E-05	serine carboxypeptidase-like 15 (SCPL15)

342	AT5G45000	-1,5101	-0,1424	9,74E-08	3,63E-06	Disease resistance protein (TIR-NBS-LRR class) family
343	AT4G12510	-1,5108	1,7979	3,30E-21	7,19E-19	Bifunctional inhibitor/lipid-transfer protein/seed storage 2S albumin superfamily protein
344	AT3G26610	-1,5109	1,6467	2,13E-19	3,88E-17	Pectin lyase-like superfamily protein
345	AT3G46300	-1,5112	-0,7070	3,32E-06	8,30E-05	unknown protein
346	AT5G26920	-1,5170	3,0398	7,13E-17	1,07E-14	CAM-BINDING PROTEIN 60-LIKE G (CBP60G)
347	AT1G60470	-1,5171	2,8804	8,62E-20	1,63E-17	galactinol synthase 4 (GolS4)
348	AT5G37478	-1,5176	-0,7532	8,32E-06	1,84E-04	TPX2 (targeting protein for Xklp2) protein family
349	AT5G25260	-1,5268	1,2281	1,36E-13	1,32E-11	SPFH/Band 7/PHB domain-containing membrane-associated protein family
350	AT5G54190	-1,5335	3,6517	2,09E-32	1,17E-29	protochlorophyllide oxidoreductase A (PORA)
351	AT1G06310	-1,5358	-0,5068	8,85E-07	2,60E-05	acyl-CoA oxidase 6 (ACX6)
352	AT3G55710	-1,5371	3,5858	7,01E-43	6,24E-40	UDP-Glycosyltransferase superfamily protein
353	AT1G04660	-1,5396	0,0637	2,17E-08	9,47E-07	glycine-rich protein
354	AT2G29130	-1,5398	1,4243	3,01E-19	5,36E-17	laccase 2 (LAC2)
355	AT1G08090	-1,5427	2,3119	1,27E-14	1,41E-12	nitrate transporter 2:1 (NRT2:1)
356	AT3G17520	-1,5442	-0,6028	2,57E-06	6,65E-05	Late embryogenesis abundant protein (LEA) family protein
357	AT4G04990	-1,5648	1,9176	1,85E-16	2,69E-14	Protein of unknown function (DUF761)
358	AT5G44120	-1,5685	-0,3150	1,62E-03	1,50E-02	CRUCIFERINA (CRA1)
359	AT2G30750	-1,6009	5,6456	1,80E-34	1,18E-31	cytochrome P450, family 71, subfamily A, polypeptide 12 (CYP71A12)
360	AT2G23270	-1,6354	-0,6232	1,19E-06	3,41E-05	unknown protein
361	AT5G62420	-1,6677	0,0531	3,12E-10	1,87E-08	NAD(P)-linked oxidoreductase superfamily protein
362	AT5G23840	-1,6721	1,8956	2,35E-26	8,09E-24	MD-2-related lipid recognition domain-containing protein
363	AT5G48430	-1,6750	2,5495	1,58E-22	3,87E-20	Eukaryotic aspartyl protease family protein
364	AT1G47890	-1,6858	-0,4473	1,97E-08	8,67E-07	receptor like protein 7 (RLP7)
365	AT1G06923	-1,6951	-0,9855	3,28E-06	8,22E-05	Similar to: ovate family protein 17
366	AT3G16670	-1,6985	4,2932	1,63E-31	8,61E-29	Pollen Ole e 1 allergen and extensin family protein
367	AT1G26410	-1,7207	1,7210	8,40E-13	7,32E-11	FAD-binding Berberine family protein
368	AT4G14630	-1,7369	3,4311	1,06E-23	2,84E-21	germin-like protein 9 (GLP9)
369	AT5G48400	-1,8203	0,3353	9,70E-15	1,11E-12	ATGLR1.2
370	AT3G62950	-1,8204	0,7386	5,07E-17	7,70E-15	Thioredoxin superfamily protein
371	AT2G35980	-1,8565	1,8498	2,88E-31	1,48E-28	YELLOW-LEAF-SPECIFIC GENE 9 (YLS9)
372	AT3G61390	-1,8581	0,5484	6,52E-16	8,94E-14	RING/U-box superfamily protein

AT4G33120	-1,8585	1,7435	2,41E-29	1,03E-26	S-adenosyl-L-methionine-dependent methyltransferases superfamily protein
AT3G06220	-1,8836	-0,9115	2,95E-07	9,74E-06	AP2/B3-like transcriptional factor family protein
AT4G31970	-1,8911	2,3145	1,26E-10	8,07E-09	cytochrome P450, family 82, subfamily C, polypeptide 2 (CYP82C2)
AT1G52790	-1,8948	-0,9856	6,69E-07	2,02E-05	contains PF03171 2OG-Fe(II) oxygenase superfamily domain
AT1G53610	-1,9288	-1,1991	3,89E-06	9,58E-05	unknown protein
AT3G21660	-1,9314	-0,4035	5,29E-10	3,08E-08	UBX domain-containing protein
AT1G49030	-1,9358	-0,7558	1,05E-08	4,81E-07	PLAC8 family protein
AT4G22214	-2,0124	1,4553	2,08E-30	9,79E-28	Defensin-like (DEFL) family protein
AT5G49870	-2,0173	-1,0526	8,32E-08	3,17E-06	Mannose-binding lectin superfamily protein
AT3G01175	-2,0224	-0,9018	2,24E-08	9,73E-07	Protein of unknown function (DUF1666)
AT4G33720	-2,0302	0,3790	3,36E-04	4,33E-03	CAP (Cysteine-rich secretory proteins, Antigen 5, and Pathogenesis-related 1 protein)
AT1G50930	-2,0389	-1,2092	1,08E-06	3,14E-05	unknown protein
AT4G11170	-2,0556	0,5013	1,34E-18	2,28E-16	Disease resistance protein (TIR-NBS-LRR class) family
AT2G19060	-2,0879	0,6011	1,15E-19	2,15E-17	SGNH hydrolase-type esterase superfamily protein
AT1G13500	-2,1453	-1,2325	6,64E-07	2,01E-05	Protein of unknown function (DUF1262)
AT4G15990	-2,1715	-0,3416	2,85E-12	2,30E-10	unknown protein
AT1G77530	-2,2366	2,6955	1,52E-60	2,72E-57	O-methyltransferase family protein
AT1G26390	-2,3131	3,7957	1,33E-17	2,17E-15	FAD-binding Berberine family protein
AT1G52820	-2,3279	2,9611	1,72E-32	9,92E-30	2-oxoglutarate (2OG) and Fe(II)-dependent oxygenase superfamily protein
AT3G21460	-2,4625	0,0957	8,27E-19	1,43E-16	Glutaredoxin family protein
AT5G38910	-2,6048	2,0703	7,04E-44	6,91E-41	RmlC-like cupins superfamily protein
AT1G58320	-2,6543	0,7670	1,15E-30	5,62E-28	PLAC8 family protein
AT1G05880	-2,6857	-1,1877	7,95E-09	3,71E-07	ARIADNE 12 (ARI12)
AT5G06900	-3,6295	-0,5686	6,05E-20	1,17E-17	cytochrome P450, family 93, subfamily D, polypeptide 1 (CYP93D1)
AT4G27570	-3,6929	-0,8894	3,07E-17	4,77E-15	UDP-Glycosyltransferase superfamily protein
AT3G05950	-3,7672	-1,3139	2,96E-13	2,75E-11	RmlC-like cupins superfamily protein
AT4G04950	-7,8621	4,2847	0,00E+00	0,00E+00	PICOT1

FC, fold change; CPM, counts per million; FDR, false discovery rate

Table S2. Identification and annotation of detected purine metabolite peaks.

Reporting metabolite data was presented according to the recommendation by Fernie et al., 2011			
Level	**Aspect**	**Information**	**Fill in**
general aspect	Type of metabolome analysis	targeted metabolite analysis	TRUE
		non-targeted metabolite class scale profiling	FALSE
		non-targeted metabolome scale profiling	FALSE
		non-targeted finger printing of mass features	FALSE
	Type of quantification	absolute or quantification	Relative quantification
	Type of reference samples	chemically defined	standard reference compounds aquired in chemical companies
		biologically defined	-
	Type of replication	analytical (same analytical sample preparation)	1
		technological (same biological preparation)	1
		biological (same experimental condition)	5
		full experiment	10
	Type of technology	reference publication	Lisec et al (2006)
	Sample preparation		chemical derivatized
		method of chromatography/separation	Lisec et al (2006)
		method of ionization	- 70 MeVolt hard ionization
		method of detection	electron impact ionization
metabolite/mass feature	Metabolite	metabolite name	see below
		metabolite sum formula	see below
		metabolite structure and public source of metabolite identifier	Metabolites were identified in comparison to database entries of authentic standards (Kopka *et al.*, 2005; Schauer *et al.*, 2005).
	Identification	identification process	manually supervized with Xculibar
		by authentic mass isotopomer added to one or all biological sample(s)	FALSE
		by authentic reference compound within a co-processed reference mixture	FALSE
		by authentic reference compound previously mapped to the analytical system	TRUE
		reference library	Metabolites were identified in comparison to spectrum of authentic standards analyzed with samples.

		type of mass spectrum	
		by match of molecular mass (single mass fragment)	YES
		by match of fragments	YES
		by match of fragmentation pattern	YES
		type of retention index	min/sec
		by match of retention time (index) to reference library	FALSE
	Quantification	type of quantification	relative peak area quantification by internal standard and sample fresh weight
	Validity testing	Recovery testing (chemical analog)	not performed
		Recovery testing (internally added mass isotopomer)	not performed
		Recovery testing (mixture of most divergent samples from the experiment)	not performed
		Test for linear range	not performed
		Limit of quantification (LOQ)	not performed
		Limit of detection (LOD)	not performed

Experiment title:	Metabolite profiles of Arabidopsis thaliana seedling, grxs mutant line
Organism/Plant species:	*Arabidopsis thaliana*
Organ/tissue:	seedling
Analytical tool:	GC/TOF-MS

Peak/compound no.- number of compound found

Ret . Time- Time expected, Tag Time Index and Time deviation

Putative Name- putative identification of the metabolite/derivative

Corresponding metabolite name in literature

Mol. Formula- molecular formula of the metabolite or its FA adduct;

Mass to charge ratio (m/z)

(S)- identification confirmed by a standard compound

I, II, III- different isomers

Identification level (A; B; C; D)- (A) standard or NMR; (B) MS/MS; (C) MS^E; (D) MS only

Experiment title:	Metabolite changes in *grxs17* mutants	
Organism/Plant species:	*Arabidopsis thaliana*	
Organ/tissue:	seedlings	
Analytical tool:	GC-TOF-MS	

Peak/compound no.- number referenced back to the main text
Ret . Time- Time expected, Tag Time Index and Time deviation
Putative Name- putative identification of the metabolite/derivative
Corresponding metabolite name in literature
Mol. Formula- molecular formula of the metabolite or its FA adduct;
Mass to charge ratio (m/z)
(S)- identification confirmed by a standard compound
I, II, III- different isomers
Identification level (A; B; C; D)- (A) standard or NMR; (B) MS/MS; (C) MS^{E}; (D) MS only

Peak/Compound no.	**Time Expected (min)**	**Putative metabolite name**	**Mol formula**	**g mol−1**	**Mass to charge ratio (m/z)**	**Identification level (A-D)**
Peak no. 1	3,83	Urea	CH4N2O	60,06	261	A
Peak no. 2	5,49	Allantoic acid	C4H8N4O4	176,13	189	A
Peak no. 3	9,9	Allantoin	C4H6N4O3	158,12	188	A
Peak no. 4	10,68	Hypoxanthine	C5H4N4O	136,11	192	A
Peak no. 5	12,01	Uric acid	C5H4N4O3	168,11	441	A
Peak no. 6	12,05	Xanthine	C5H4N4O2	152,11	353	A
Peak no. 7	15,09	Xanthosine	C10H12N4O6	284,23	245	A

3

Table S3. Primers used in this study.

For cloning	
attB1-GRXS17	5’-GGGGACAAGTTTGTACAAAAAAGCAGGCTCCATGAGCGGTACGGTGAAG-3’
attB2-GRXS17	5’-GGGGACCACTTTGTACAAGAAAGCTGGGTCTCMCTCGGATAGAGTTGCTTTG-3’
attB1-AtDRE2	5’-GGGGACAAGTTTGTACAAAAAAGCAGGCTCCATGGATTCGATGATGAATCA-3’
attB2-AtDRE2	5’-GGGGACCACTTTGTACAAGAAAGCTGGGTCTCMTATGTCAGCTTCAAGGAA-3’
attB1 AtXDH1	5’-GGGGACAAGTTTGTACAAAAAAGCAGGCTCCATGGGTTCACTGAAAAAGG-3’
attB2 AtXDH1	5’-GGGGACCACTTTGTACAAGAAAGCTGGGTCTCMAACACTAAGATTAGGGTAGAAATC-3’
attB1-CTU1	5’-GGGGACAAGTTTGTACAAAAAAGCAGGCTCCATGGAGGCCAAGAAC-3’
attB2-CTU1	5’-GGGGACCACTTTGTACAAGAAAGCTGGGTCTCMGAAATCCAGAGATCC-3’
attB1-CTU2	5’-GGGGACAAGTTTGTACAAAAAAGCAGGCTCCATGGCTTGTAATTCCTC-3’
attB2-CTU2	5’-GGGGACCACTTTGTACAAGAAAGCTGGGTCTCMGACAACCTCTTCATC-3’
For genotyping	
SALK_021301 grxs17-1-F	5’-CTTTCGCATTCTCCTTCACAG-3’
SALK_021301 grxs17-1-R	5’-CCTTCTCCCTCTTCGAAGATG-3’
LB SALK T-DNA primer	5’-ATTTTGCCGATTTCGGAAC-3’
GK_709D04 rol5-2-F	5’-TCGTCGGAGTTGGATCAATAG-3’
GK_709D04 rol5-2-R	5’-TGGAGAAGTAATCCAGCTTCTTG-3’
GK_686B10 ctu2-2-F	5’-CTTCGACGATGGAAGATTCTG-3’
GK_686B10 ctu2-2-R	5’-TCGAAGTGGAAGTACAATGGG-3’
GK-555H06 elo3-6-F	5’-ACCGTAAATCAGCATTTGTCG-3’
GK-555H06 elo3-6-R	5’-TGGGGTTTAGGTAGTTTTGGG-3’
GK T-DNA primer (LB)	5’-CCCATTTGGACGTGAATGTAGACA-3’C
For qRT-PCR	
GRXS17-F	5’-CGCCAAGGCCTTAAAGTGTA-3’
GRXS17-R	5’-CATAAGCTCGCCTTTCACG-3’
PARP2-F	5’-ATGGCGTTCTGCTCCTCTGC-3’
PARP2-R	5’-GGTGCTGTTTTCCCCACACC-3’
AT1G36180 ACC2-F	5’-CATGGAGTGGTTCCCATGTT-3’
AT1G36180 ACC2-R	5’-CCTCGGGGACAGTTACCA-3’
AT2G18193-F	5’-TCACCCTCAAAACCTTCCTG-3’
AT2G18193-R	5’-TTCCATATGCCTGCACTGTC-3’
AT5G24280 GMI1-F	5’-ATACGTCTTGATGACGGTTCTG-3’
AT5G24280 GMI1-R	5’-CGGTGTCAAATCCCACAAGT-3’
AT5G60250 C3H4-F	5’-TCTTATCCGATTTTCCAATACGTC-3’
AT5G60250 C3H4-R	5’-TGTTGCATGATGCTTTGAAGA-3’
AT2G04050 DTX3-F	5’-CCACAATGGTGAGCTCCAG-3’
AT2G04050 DTX3-R	5’-CACCCGCTAACCCAAACA-3’
AT3G01600 NAC044-F	5’-TCACCCTCAAAACCTTCCTG-3’
AT3G01600 NAC044-R	5’-TTCCATATGCCTGCACTGTC-3’